Le *et al. Robomech J (2016) 3:25*
DOI 10.1186/s40648-016-0063-1

ROBOMECH Journal

RESEARCH ARTICLE Open Access

Configuration of redundant drive wire mechanism using double actuator modules

Tam Nhat Le*†, Hiroki Dobashi† and Kiyoshi Nagai†

Abstract

A new wire mechanism called "redundant drive wire mechanism" (RDWM), driven by double actuator modules (DAMs) is introduced. When RDWM is used for producing multi-directional motions using DAMs, the number of wires increases and the wire matrix would become complicated. This makes finding and checking the candidates difficult. Therefore, we introduce an easier and simpler approach for judging RDWM candidates, which includes two procedures: conversion of the wire matrix to a new form, and judgment of candidates using the essential component of the new form of wire matrix related to the global motion. This paper shows a fast and convenient method for judging whether an RDWM candidate can produce the resultant forces needed to achieve required motions. The examples demonstrate the validity of the new method in dealing with RDWM candidates containing many wires.

Keywords: Wire mechanism, Redundant drive, Double actuator module, RDWM

Background

Development of parallel mechanism for high acceleration and high precision motions for industrial applications has been a focus of research for a long period of time. Wire mechanism has structure of parallel mechanism and it has been developed to produce high acceleration because of the small inertial moment of the top plate. For example, a high-speed manipulator using wire driven method called "FALCON" was proposed [1], which attained a peak acceleration of 43 G. The redundant drive concept was applied in a parallel mechanism to produce a large resultant force. In [2], a mechanism called "NINJA" was proposed; this was made light-weight by arranging the motors on a base. Its top plate with six degrees of freedom (DOF) was driven by four sub-arms with a parallel link structure. An optimum method was proposed to find the design parameters of the mechanism while reducing the inertia of the top plate. In experiments, the computation from encoders shows that NINJA can achieve an acceleration of $\geq$100 G. A high speed parallel mechanism for electronic part mounters, known as "constrained differential drive mechanism" (CDDM), was introduced [3]. In this research, a typical four DOFs pick-and-place motion was analyzed, and the trajectory was divided into two regions A and B. In region A, high precision motions were produced, whereas high acceleration motions were produced in region B. Thereafter, the virtual force redundancy (VFR) concept was introduced to the design of the high-speed parallel mechanism using CDDM. The experimental results showed that the mechanism could achieve an acceleration of $\geq$20 G. Recently, a mechanism known as "Capturing robot" which could achieve 100 G was introduced [4]. To achieve that high acceleration, spring energy was utilized in the pre-shaping dynamics of link fingers. However, this robot could only give high acceleration motion in one direction when moving to grasp object.

On the other hand, ways of changing the position and orientation of the top plate have also been studied. Because a large translational motion is required while only a small rotational motion is needed, the standard method is to maintain the translational motion while fixing the orientation of the top plate and installing an arm on it. A method with a contour crafting construction system for automated construction of civil structure known as "contour crafting cartesian cable robot" (C^4) has been proposed [5, 6], wherein the cables are mounted in pairs,

*Correspondence: letamritsumei@gmail.com
†Tam Nhat Le, Hiroki Dobashi and Kiyoshi Nagai contributed equally to this work
Department of Robotics, College of Science and Engineering, Ritsumeikan University, 1-1-1 Noji-higashi, 525-8577 Kusatsu, Shiga, Japan

and the two cables in each pair are controlled to have the same length. A parallelogram is then formed by each pair of cables, the corresponding crossbar and end-effector edge. By maintaining this parallelism, the orientation of the top plate remains fixed and only translational motion is possible. The research [5] presented the kinematics and statics of the proposed method while the research [6] presented the dynamics and developed a controller of the system. Though the working principle is not mechanical, it heavily depends on the controller. Realizing this idea, the research introduced the design method of a cable-driven robot with translational motion focusing on the tension condition in the cables then showed a prototype of the system [7]. Using a similar approach, the designers of "Beta Bot" developed a mechanism with six cables and a spine in the middle of the end effector [8]. The six cables were grouped into three pairs, and the two wires in each pair were connected to one side of the end-effector. The other ends of the two wires were then wound onto two pulleys driven by the same actuator. The two wires, together with the line which connected the two contact points on the pulleys and the end-effector edge, formed a parallelogram. The three parallelograms ensured that the end-effector would only perform three translational motions, with no change in orientation. The design of "Beta Bot" halved the number of actuators presented in [5]. In contrast to the idea of maintaining the parallelism of wires to fix the orientation of the top plate as the above researches, the authors in [9] developed a power assist device to help elderly patients and patients with disabilities in moving, without using the parallelism of wires while fixing the orientation of the supporting element. The device contained the upper part and the lower part. The upper part could produce the translational motion in the horizontal only using a set A including three wires strung at the same length and a set B including two wires strung at the same length. The lower part contained three pairs of wires, two wires in a pair were reeled in and out to have the same length by the three corresponding actuators put on the upper part. By using these three pairs of wires, the lower part could move with three degrees of freedom in the vertical plane for the motions of standing up and sitting down of the user. The lower part could also perform a rotation motion around the vertical axis w.r.t the upper part using a connecting part between the upper part and the lower part to help the user in changing the moving direction. Another approach changed the orientation of the end-effector and installed arms on the top plate [10–12]. The orientation of the end effector could be changed by changing the position of the arm. However, the placement of the actuators on the top plate gave the mechanism high inertia. One way to reduce the inertia of the top plate is to introduce a parallel module such as "DELTA" [13] or "HEXA" [14] into the the top plate of wire mechanism.

To develop a parallel wire mechanism with high acceleration and high precision motions using the redundant drive concept, we proposed a mechanism called "redundant drive wire mechanism" (RDWM) [15]. The goal of this research was to develop a wire mechanism capable of high acceleration using only the translational motion that could also perform high-precision local motions in 3D space. This research introduced a wire mechanism using double actuator modules (DAMs) and internal DOFs to produce global coarse motion with high acceleration and local motion with high precision. In [16–18], velocity constraint modules (VCMs) were introduced to reduce the number of actuators, to produce translational motion, and to fix the orientation of the top plate in an RDWM.

When constructing an RDWM, it is necessary to judge whether the mechanism can produce the resultant force in all directions. Since the number of actuators in an RDWM is large, especially in the 3D case, the size of the wire matrix also becomes large. This creates difficulties in judging the configuration of the mechanism using the conventional method. In our approach, the wire matrix is based on the structure of the DAM, and only the essential component is used to judge the configuration of the RDWM.

In this paper, we present a method for judging whether a candidate RDWM can produce the resultant forces necessary for achieving the required motions. The paper is organized as follows. First, the basic concept of RDWM is presented, and some candidate mechanisms are proposed. Second, a method for deriving the wire matrix of an RDWM based on DAMs in normal expression is presented. Third, a new method for judging candidate RDWMs is introduced, including a new form of wire matrix. The proposed judgment of candidates uses the essential component of the new form. This component has the size equal to only a quarter of the size of the wire matrix; hence, it makes finding and checking candidate RDWMs to be easier and simpler. Next, numerical examples of RDWM in 2D and 3D cases are introduced to test the validity of the new method in checking vector closure condition. Designing the configuration of an RDWM is then discussed. Finally, the findings of the research are summarized in the conclusions section.

Basic concept for developing a redundant drive wire mechanism

Figure 1 shows that fast motion and high precision motion are not simultaneously required. The pick-and-place motion can therefore be divided into two separate stages. In this figure, the top plate can move an object

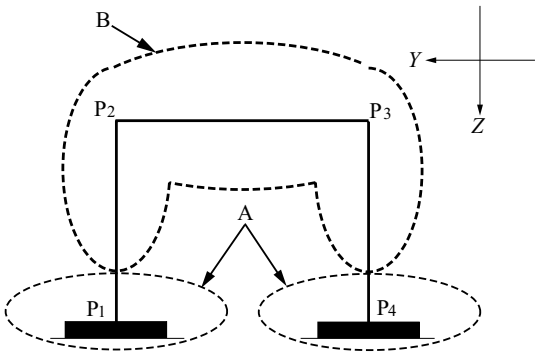

Fig. 1 Pick and place motion [3]

from point P_1 to P_4 following the trajectory P_1–P_2–P_3 P_4. For time reduction, all the motions in region B should be kept short. In contrast, all the motions in region A must be precise.

The concept of RDWM uses DAMs to produce high acceleration and high precision motions. The DAM contains two actuators that move the top plate and rotate the local pulley, as shown in Fig. 2. Actually, there is a research introduces about DAMs [19], however the research focuses on the rotational motions to control their tendon-driven robotic hand without any utilization of the translational motion for producing fast motion. In this proposed DAM, when the two actuators rotate in the same direction, the translational motion is produced as global motion. Then, when the two actuators rotate in different directions, local motion will be produced by the rotation of the local pulley, this is utilized to perform precision motion. In this schematic figure, the points $\boldsymbol{A}_{i1}$, $\boldsymbol{A}_{i2}$, $\boldsymbol{B}_{i1}$, $\boldsymbol{B}_{i2}$ are shown as holes for making the figure to be simple; however, in the real mechanism, some small

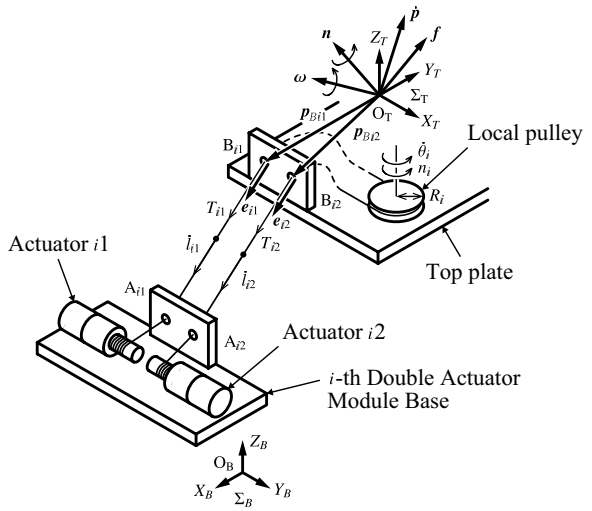

Fig. 2 Double actuators module

pulley systems need to be introduced into the DAM and into the top plate such that those points are the tangential points between wires and the outlet pulleys. An example of the pulley system to reduce the affect of friction is shown in Fig. 13. This system allows the wire to change its direction in response to the posture of the top plate and therefore it helps to reduce the affect of friction.

The wire mechanism has the ability to move an object in a wide range of motions using translational motion. To change the orientation of an object, only a small range of motion is required. Translational motions are used to realize global fast motion only when the orientation can be fixed. Local motions are then used to change the orientation of the manipulator and realize precision motions. Figure 3 shows that in the RDWM, the top plate is controlled by 14 wires in seven DAMs. It can move through a large working space with fast motion and can also undertake specific tasks with highly precise motion using the three fingers on the top plate. The three fingers can perform grasping tasks using a common DOF, and can hold the object using two DOFs for each finger.

Wire matrix and problem statement

Derivation of wire matrix

In the ith DAM shown in Fig. 2, ${}^B\dot{\boldsymbol{p}}_{Bij}$ is the velocity of the wire end points on the top plate w.r.t the base coordinate, ${}^B\dot{\boldsymbol{p}}_T$ is the velocity of the center of the top plate w.r.t the base coordinate, ${}^B\boldsymbol{\omega}$ is the angular velocity of the top plate, and ${}^B\boldsymbol{p}_{Bij}$ is the position of the wire end points on the top plate w.r.t the base coordinate. The following relationships can then be obtained:

$$ {}^B\dot{\boldsymbol{p}}_{Bij} = {}^B\dot{\boldsymbol{p}}_T + {}^B\boldsymbol{\omega} \times {}^B\boldsymbol{p}_{Bij}, \quad i = 1,\ldots,N;\ j = 1,2 \tag{1} $$

The operator $\times$ in Eq. (1) represents the cross product of two vectors ${}^B\boldsymbol{\omega}$ and ${}^B\boldsymbol{p}_{Bij}$. The wire velocities are given by

$$ \begin{cases} \dot{l}_{i1} = {}^B\boldsymbol{e}_{i1}^{\mathrm{T}}\,{}^B\dot{\boldsymbol{p}}_{Bi1} + R_i\dot{\theta}_i, \\ \dot{l}_{i2} = {}^B\boldsymbol{e}_{i2}^{\mathrm{T}}\,{}^B\dot{\boldsymbol{p}}_{Bi2} - R_i\dot{\theta}_i, \end{cases} \tag{2} $$

where $\dot{l}_{i1}$, $\dot{l}_{i2}$ are the wire velocities, ${}^B\boldsymbol{e}_{i1}$, ${}^B\boldsymbol{e}_{i2}$ are the wire vectors with unit length, R_i is the radius of the pulley, and $\dot{\theta}_i$ is the angular velocity of the pulley.

Substituting Eq. (1) into Eq. (2) and applying the scalar triple product gives

$$ \begin{bmatrix} \dot{l}_{i1} \\ \dot{l}_{i2} \end{bmatrix} = \begin{bmatrix} {}^B\boldsymbol{e}_{i1}^{\mathrm{T}} & ({}^B\boldsymbol{p}_{Bi1} \times {}^B\boldsymbol{e}_{i1})^{\mathrm{T}} & R_i \\ {}^B\boldsymbol{e}_{i2}^{\mathrm{T}} & ({}^B\boldsymbol{p}_{Bi2} \times {}^B\boldsymbol{e}_{i2})^{\mathrm{T}} & -R_i \end{bmatrix} \begin{bmatrix} {}^B\dot{\boldsymbol{p}}_T \\ {}^B\boldsymbol{\omega} \\ \dot{\theta}_i \end{bmatrix}. \tag{3} $$

Applying duality, the resultant force caused by T_{i1} and T_{i2} are:

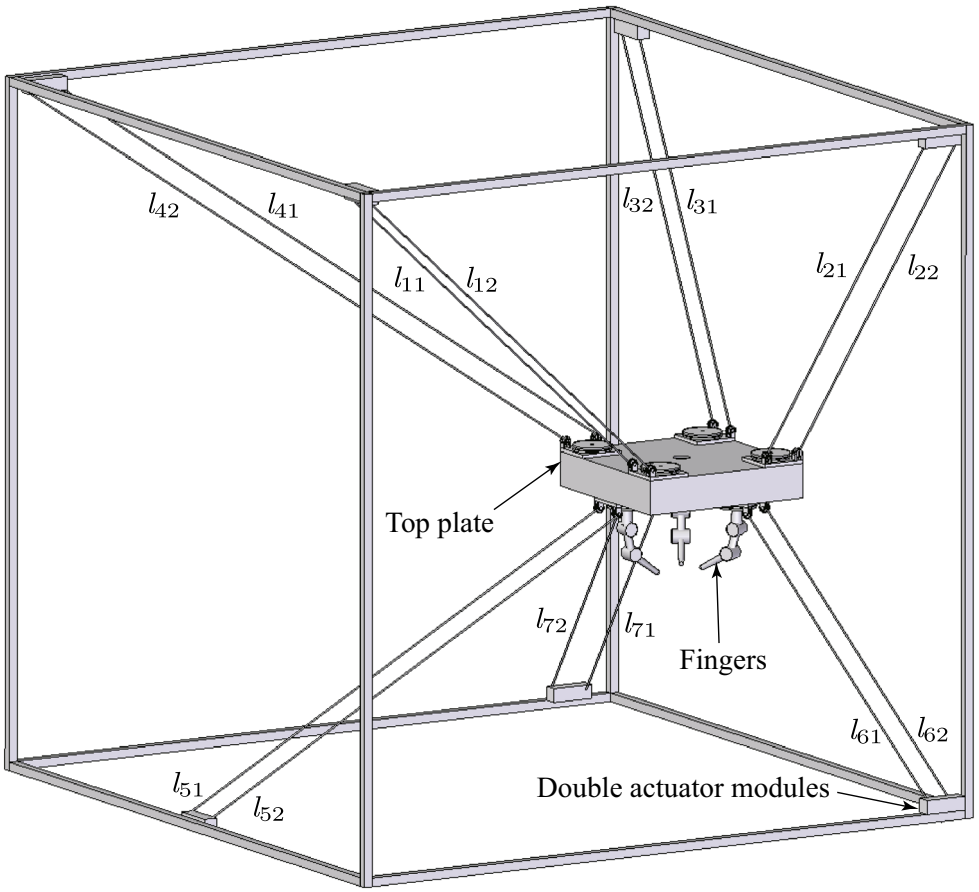

Fig. 3 An image of the target wire mechanism

$$\begin{bmatrix} {}^{B}\boldsymbol{f}_i \\ {}^{B}\boldsymbol{n}_i \\ \boldsymbol{n}_i \end{bmatrix} = \begin{bmatrix} {}^{B}\boldsymbol{e}_{i1} & {}^{B}\boldsymbol{e}_{i2} \\ {}^{B}\boldsymbol{p}_{Bi1} \times {}^{B}\boldsymbol{e}_{i1} & {}^{B}\boldsymbol{p}_{Bi2} \times {}^{B}\boldsymbol{e}_{i2} \\ R_i & -R_i \end{bmatrix} \begin{bmatrix} T_{i1} \\ T_{i2} \end{bmatrix}. \quad (4)$$

When the wire mechanism containing N DAMs is considered in the n directional space, the relationship between the resultant force vector and the wire tension vector is given by

$$\boldsymbol{F} = \boldsymbol{W}\boldsymbol{T}, \quad (5)$$

where $\boldsymbol{T} = \left[T_{11} \;\; T_{12} \;\; T_{21} \;\; T_{22} \;\; ... \;\; T_{N1} \;\; T_{N2} \right]^{\mathrm{T}}_{2N\times 1}$ is the wire tension vector, $\boldsymbol{F}(=\left[f_x \; f_y \; f_z \; n_x \; n_y \; n_z \; n_1 \; \ldots \; n_N \right]^{\mathrm{T}}_{(n+N)\times 1}$ in the case of $n = 6$) is the resultant force vector, $\boldsymbol{W}$ is the wire matrix defined as

$$\boldsymbol{W} = \begin{bmatrix} \boldsymbol{W}_A \\ \boldsymbol{W}_B \end{bmatrix}_{(n+N)\times 2N}. \quad (6)$$

Here, the size of the wire matrix $\boldsymbol{W}$ is $(n+N)\times 2N$, where $(n+N)$ is the number of rows and includes n DOFs in the global motion space and N DOFs in the local motion space. The number of columns is $2N$, which is two times the number of DOFs in the local motion space. The matrix $\boldsymbol{W}$, which contains the matrix $\boldsymbol{W}_A$ contributing to the resultant force exerted on the top plate, and the matrix $\boldsymbol{W}_B$ contributing to the local moments of the local pulleys. The two matrices are as follows:

$$\boldsymbol{W}_A = \begin{bmatrix} {}^{B}\boldsymbol{e}_{11} & {}^{B}\boldsymbol{e}_{12} & {}^{B}\boldsymbol{e}_{21} & {}^{B}\boldsymbol{e}_{22} & \cdots & {}^{B}\boldsymbol{e}_{N1} & {}^{B}\boldsymbol{e}_{N2} \\ {}^{B}\boldsymbol{p}_{B11} \times {}^{B}\boldsymbol{e}_{11} & {}^{B}\boldsymbol{p}_{B12} \times {}^{B}\boldsymbol{e}_{12} & {}^{B}\boldsymbol{p}_{B21} \times {}^{B}\boldsymbol{e}_{21} & {}^{B}\boldsymbol{p}_{B22} \times {}^{B}\boldsymbol{e}_{22} & \cdots & {}^{B}\boldsymbol{p}_{BN1} \times {}^{B}\boldsymbol{e}_{N1} & {}^{B}\boldsymbol{p}_{BN2} \times {}^{B}\boldsymbol{e}_{N2} \end{bmatrix}_{n\times 2N}, \quad (7)$$

$$\boldsymbol{W}_B = \begin{bmatrix} R_1 & -R_1 & 0 & 0 & \cdots & 0 & 0 \\ 0 & 0 & R_2 & -R_2 & \cdots & 0 & 0 \\ \vdots & \vdots & \vdots & \vdots & \vdots & \vdots & \vdots \\ 0 & 0 & 0 & 0 & \cdots & R_N & -R_N \end{bmatrix}_{N\times 2N}. \quad (8)$$

Problem statement

The matrix $\boldsymbol{W}$ with size $(n+N)\times 2N$ becomes very large when developing wire mechanisms using a large number of DAMs to move in a multi-directional space. This is inconvenient, making it difficult to judge whether the wire mechanism has a proper configuration using standard approaches. A method for dealing with large wire matrices is therefore necessary for developing a multi-directional RDWM.

Configuration of an RDWM

Conversion of wire matrix

The proposed method consists of two procedures. The procedure for converting the wire matrix by considering the sums and differences of the sets of two wire tensions of the DAMs is described first. The procedure for judging a candidate mechanism using the components of the wire matrix that relate the resultant forces and the combination of the sums of the sets of two wire tensions of the DAMs is presented in the following section.

Defining ${}^T\boldsymbol{p}_{TCi}$, R_i, ${}^T\boldsymbol{p}_{TDi}$ and ${}^T\boldsymbol{p}_{Bij}$

Figure 4 shows the relations between the parameters of a DAM. Here, ${}^T\boldsymbol{p}_{TCi}$ is the position vector of the center point $\boldsymbol{C}_i$ of $\boldsymbol{B}_{i1}\boldsymbol{B}_{i2}$ w.r.t the top plate's center $\boldsymbol{O}_T$; ${}^T\boldsymbol{p}_{Bi1}$ and ${}^T\boldsymbol{p}_{Bi2}$ are the position vectors of $\boldsymbol{B}_{i1}$ and $\boldsymbol{B}_{i2}$ w.r.t $\boldsymbol{O}_T$; ${}^T\boldsymbol{p}_{TDi}$ is the position vector of $\boldsymbol{B}_{i1}$ w.r.t $\boldsymbol{C}_i$, and it has the norm equal to the pulley radius R_i. As shown in the figure, the three vectors ${}^T\boldsymbol{p}_{Bi1}$, ${}^T\boldsymbol{p}_{TCi}$ and ${}^T\boldsymbol{p}_{TDi}$ create a triangle; the three vectors ${}^T\boldsymbol{p}_{Bi2}$, ${}^T\boldsymbol{p}_{TCi}$ and ${}^T\boldsymbol{p}_{TDi}$ also create a triangle; therefore the below relations can be derived:

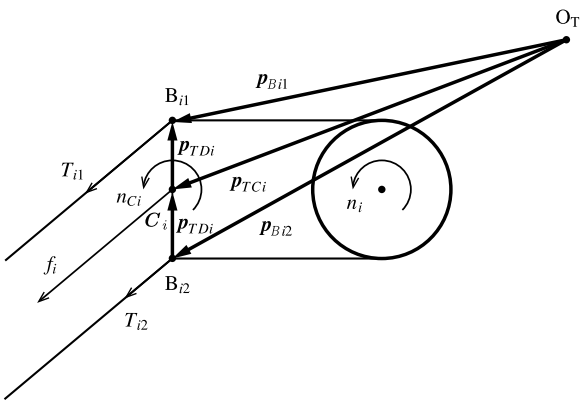

Fig. 4 The set of force and moment equivalent to a set of wire tensions applied to a DAM

$$\begin{cases} {}^T\boldsymbol{p}_{Bi1} = {}^T\boldsymbol{p}_{TCi} + {}^T\boldsymbol{p}_{TDi}, \\ {}^T\boldsymbol{p}_{Bi2} = {}^T\boldsymbol{p}_{TCi} - {}^T\boldsymbol{p}_{TDi}. \end{cases} \quad (9)$$

Set of position ${}^B\boldsymbol{p}_T$ and orientation ${}^B\boldsymbol{R}_T$ of the top plate

The initial position ${}^B\boldsymbol{p}_T$ and orientation ${}^B\boldsymbol{R}_T$ of the top plate can have an arbitrary value inside the working space of the top plate.

Position of wire end points on the top plate

This is given by the following equation:

$${}^B\boldsymbol{p}_{Bij} = {}^B\boldsymbol{p}_T + {}^B\boldsymbol{R}_T\,{}^T\boldsymbol{p}_{Bij}, \quad (10)$$

where ${}^B\boldsymbol{R}_T$ is the rotational matrix from the base coordinate to the top coordinate.

Position of wire end points on the frame

The positions of the wire end points on the frame ${}^B\boldsymbol{p}_{Aij}$ need to be chosen so that the wire vectors span the motion direction of the top plate.

Calculating the wire vectors ${}^B\boldsymbol{e}_{ij}$

The wire vectors can be derived from the following equation:

$${}^B\boldsymbol{e}_{ij} = \frac{{}^B\boldsymbol{p}_{Aij} - {}^B\boldsymbol{p}_{Bij}}{\|{}^B\boldsymbol{p}_{Aij} - {}^B\boldsymbol{p}_{Bij}\|}. \quad (11)$$

Here, ${}^B\boldsymbol{p}_{Aij} = \begin{bmatrix} {}^Bx_{Aij} & {}^By_{Aij} & {}^Bz_{Aij} \end{bmatrix}^{\mathrm{T}}$ are the positions of the wire end points on the frame w.r.t the base coordinate and ${}^B\boldsymbol{p}_{Bij} = \begin{bmatrix} {}^Bx_{Bij} & {}^By_{Bij} & {}^Bz_{Bij} \end{bmatrix}^{\mathrm{T}}$ represents the positions of the wire end points on the top plate w.r.t the base coordinate. The symbol $\|\cdot\|$ in Eq. (11) represents the Euclidean norm of a vector.

Checking if the two wires in a DAM are in parallel

Because the top plate can change its orientation when the system is operating, there will have cases where the two wires in a DAM are twisted and contacted with each other, which make bad affect to the operation of RDWM. This paper assumes that the change of the orientation of the top plate is small enough and the set of two wires of DAM can be treated to be parallel. The method to fix the orientation of the top plate to ensure this assumption will be discussed in another topic.

Derivation of the wire matrix in normal form

The derivation of the wire matrix in normal form is shown in Eqs. (6), (7), and (8).

Derivation of the wire matrix in new form

With the structure of DAM shown in Fig. 4, the two wires in each DAM are in parallel so the two wire vectors ${}^B\boldsymbol{e}_{i1}$,

${}^{B}\boldsymbol{e}_{i2}$ can be represented as one vector ${}^{B}\boldsymbol{e}_{i}$ with the same direction at the center point $\boldsymbol{C}_i$. Then ${}^{B}\boldsymbol{e}_{i}$ can be derived as follows:

$$ {}^{B}\boldsymbol{e}_{i} = {}^{B}\boldsymbol{e}_{ij}. \tag{12} $$

The vectors ${}^{B}\boldsymbol{p}_{TCi}$ and ${}^{B}\boldsymbol{p}_{TDi}$ are derived from the position of points $\boldsymbol{B}_{ij}$ as follows:

$$ \begin{cases} {}^{B}\boldsymbol{p}_{TCi} = ({}^{B}\boldsymbol{p}_{Bi1} + {}^{B}\boldsymbol{p}_{Bi2})/2, \\ {}^{B}\boldsymbol{p}_{TDi} = ({}^{B}\boldsymbol{p}_{Bi1} - {}^{B}\boldsymbol{p}_{Bi2})/2. \end{cases} \tag{13} $$

Then Eq. (4) becomes

$$ \begin{bmatrix} {}^{B}\boldsymbol{f}_{i} \\ {}^{B}\boldsymbol{n}_{i} \\ \boldsymbol{n}_{i} \end{bmatrix} = \begin{bmatrix} {}^{B}\boldsymbol{e}_{\mathrm{i}} & 0 \\ {}^{B}\boldsymbol{p}_{TC\mathrm{i}} \times {}^{B}\boldsymbol{e}_{i} & {}^{B}\boldsymbol{p}_{TDi} \times {}^{B}\boldsymbol{e}_{i} \\ 0 & R_i \end{bmatrix} \begin{bmatrix} T_{i1} + T_{i2} \\ T_{i1} - T_{i2} \end{bmatrix}. \tag{14} $$

The expressions in Eqs. (5) and (6) can be converted into a new expression as

$$ \boldsymbol{F} = \boldsymbol{W}^{'}\boldsymbol{T}^{'}. \tag{15} $$

Here, $\boldsymbol{T}^{'} = \begin{bmatrix} \boldsymbol{T_S} & \boldsymbol{T_D} \end{bmatrix}^{\mathrm{T}}_{2N\times 1}$ is the new expression of the wire tension vector, $\boldsymbol{T_S} = \begin{bmatrix} (T_{11} + T_{12}) & \cdots & (T_{N1} + T_{N2}) \end{bmatrix}^{\mathrm{T}}_{N\times 1}$ is the vector of the sums of the sets of two wire tensions of the DAMs, and $\boldsymbol{T_D} = \begin{bmatrix} (T_{11} - T_{12}) & \cdots & (T_{N1} - T_{N2}) \end{bmatrix}^{\mathrm{T}}_{N\times 1}$ is the vector of the differences of the sets of two wire tensions of the DAMs. The new expression of wire matrix $\boldsymbol{W}^{'}$ is given by

$$ \boldsymbol{W}^{'} = \begin{bmatrix} \boldsymbol{W}^{'}_{A} & \boldsymbol{W}_{C} \\ \boldsymbol{O} & \boldsymbol{W}^{'}_{B} \end{bmatrix}_{(n+N)\times 2N}. \tag{16} $$

Inside the matrix $\boldsymbol{W}^{'}$, the matrix $\boldsymbol{W}^{'}_{B}$ contributes to producing local moments of pulleys on the top plate while the set of matrices $\boldsymbol{W}^{'}_{A}$ and $\boldsymbol{W}_{C}$ contributes to producing the resultant force and resultant moment on the top plate. The contents of $\boldsymbol{W}^{'}_{A}$, $\boldsymbol{W}^{'}_{B}$, and $\boldsymbol{W}_{C}$ are shown below:

$$ \boldsymbol{W}^{'}_{A} = \begin{bmatrix} {}^{B}\boldsymbol{e}_{1} & {}^{B}\boldsymbol{e}_{2} & \cdots & {}^{B}\boldsymbol{e}_{N} \\ {}^{B}\boldsymbol{p}_{TC1} \times {}^{B}\boldsymbol{e}_{1} & {}^{B}\boldsymbol{p}_{TC2} \times {}^{B}\boldsymbol{e}_{2} & \cdots & {}^{B}\boldsymbol{p}_{TCN} \times {}^{B}\boldsymbol{e}_{N} \end{bmatrix}_{n\times N}, \tag{17} $$

$$ \boldsymbol{W}^{'}_{B} = \begin{bmatrix} R_1 & 0 & \cdots & 0 \\ 0 & R_2 & \cdots & 0 \\ \vdots & \vdots & \vdots & \vdots \\ 0 & 0 & \cdots & R_N \end{bmatrix}_{N\times N}, \tag{18} $$

$$ \boldsymbol{W}_{C} = \begin{bmatrix} \boldsymbol{O} \\ \boldsymbol{p}_{TD1} \times {}^{B}\boldsymbol{e}_{1} \;\; \boldsymbol{p}_{TD2} \times {}^{B}\boldsymbol{e}_{2} \;\; \cdots \;\; \boldsymbol{p}_{TDN} \times {}^{B}\boldsymbol{e}_{N} \end{bmatrix}_{n\times N}. \tag{19} $$

The converted matrix $\boldsymbol{W}^{'}$ describes the geometrical meaning of the sums and differences of the sets of two wire tensions of the DAMs. In Fig. 4, the set of wire tensions $[T_{i1}, T_{i2}]$ is equivalent to the set of force and moment $[f_i, n_{Ci}]$ derived from the sum $(T_{i1} + T_{i2})$ and difference $(T_{i1} - T_{i2})$. The component ${}^{B}\boldsymbol{p}_{TCi} \times {}^{B}\boldsymbol{e}_{i}$, which produces the moment at the center of the top plate comes from the sum $(T_{i1} + T_{i2})$ while the component ${}^{B}\boldsymbol{p}_{TDi} \times {}^{B}\boldsymbol{e}_{i}$ produces the moment at the center of $\mathrm{B}_{i1}\mathrm{B}_{i2}$ from the difference $(T_{i1} - T_{i2})$.

Judgment of a candidate

The procedure for judging whether a candidate RDWM can produce the resultant forces for achieving the required motions is discussed in this section. Figure 5a shows the wire vectors on the top plate with four sets of DAMs. When two wires in the DAM are in parallel, the two wire vectors ${}^{B}\boldsymbol{e}_{i1}$ and ${}^{B}\boldsymbol{e}_{i2}$ can be expressed as a common vector in the center of $\mathrm{B}_{i1}\mathrm{B}_{i2}$ labeled ${}^{B}\boldsymbol{e}_{i}$ as shown in Fig. 5b.

We found that in order to check the ability for producing force in any direction, it is not necessary to evaluate the whole matrix $\boldsymbol{W}$. Instead, matrix $\boldsymbol{W}$ is converted into matrix $\boldsymbol{W}^{'}$. Although the two matrices are of the same size, this matrix is already divided into small components by Eq. (16), and only the matrix $\boldsymbol{W}^{'}_{A}$ relating to the global motion needs to be checked for vector closure condition. Note that neither of the matrix $\boldsymbol{W}$ nor the matrix $\boldsymbol{W}^{'}$ is necessary to be derived from now. What we need to do is to derive ${}^{B}\boldsymbol{e}_{i}$ and ${}^{B}\boldsymbol{p}_{TCi}$ then substitute them to Eq. (17) to get matrix $\boldsymbol{W}^{'}_{A}$ for the process of judgment of a candidate. Matrix $\boldsymbol{W}^{'}_{A}$ has size $n \times N$ with rows equal to the number of DOF n of the motion space and columns equal to the number of DAMs N. This is a quarter of the size of the matrix $\boldsymbol{W}$, making the judgment much more convenient.

From the statics relationship between wire tensions and the resultant force in Eq. (5), the new expression of statics relations is given by Eq. (15). The resultant force and moment on the top plate are given by

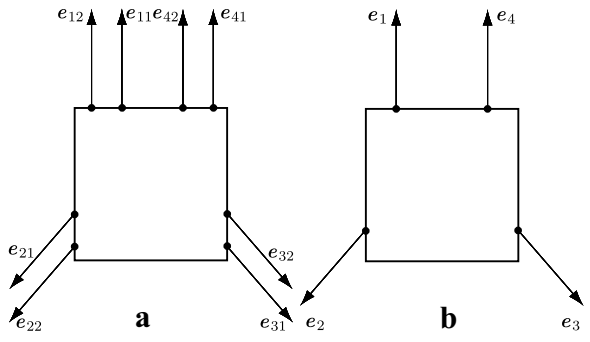

Fig. 5 Wire vectors on the top plate with DAMs and the simple expression **a** shows the wire vectors on the top plate with DAMs and **b** shows the simple expression of wire vectors

$$\begin{bmatrix} f_x \\ f_y \\ f_z \\ n_x \\ n_y \\ n_z \end{bmatrix} = \begin{bmatrix} \boldsymbol{W}'_{Af} \\ \boldsymbol{W}'_{Am} \end{bmatrix} \boldsymbol{T_S} + \begin{bmatrix} \boldsymbol{O} \\ \boldsymbol{W}_{Cnz} \end{bmatrix} \boldsymbol{T_D}, \tag{20}$$

where:

$$\boldsymbol{W}'_{Af} = \begin{bmatrix} {}^B\boldsymbol{e}_1 & {}^B\boldsymbol{e}_2 & \cdots & {}^B\boldsymbol{e}_N \end{bmatrix}_{n_f \times N} \tag{21}$$

is the part of matrix $\boldsymbol{W}'_A$ in Eq. (17) which is related to the resultant force on the top plate;

$$\boldsymbol{W}'_{Am} = \begin{bmatrix} {}^B\boldsymbol{p}_{TC1} \times {}^B\boldsymbol{e}_1 & {}^B\boldsymbol{p}_{TC2} \times {}^B\boldsymbol{e}_2 & \cdots & {}^B\boldsymbol{p}_{TCN} \times {}^B\boldsymbol{e}_N \end{bmatrix}_{n_m \times N} \tag{22}$$

is the part of matrix $\boldsymbol{W}'_A$ which is related to the resultant moment on the top plate;

$$\boldsymbol{O} = [0]_{n_f \times N} \tag{23}$$

is an $n_f \times N$ zero matrix;

$$\boldsymbol{W}_{Cnz} = \begin{bmatrix} \boldsymbol{p}_{TD1} \times {}^B\boldsymbol{e}_1 & \boldsymbol{p}_{TD2} \times {}^B\boldsymbol{e}_2 & \cdots & \boldsymbol{p}_{TDN} \times {}^B\boldsymbol{e}_N \end{bmatrix}_{n_m \times N} \tag{24}$$

is the non-zero part of matrix $\boldsymbol{W}_C$ in Eq. (19). Here, $n_f + n_m = n$, where n_f is the number of DOFs under the resultant force, n_m is the number of DOFs under the resultant moment and n is the total number of DOFs of the whole motion space.

From Eq. (20), the resultant moment can be derived as

$$\boldsymbol{n} = \boldsymbol{n_S} + \boldsymbol{n_D}. \tag{25}$$

Here, $\boldsymbol{n} = [n_x \ n_y \ n_z]^{\mathrm{T}}$ is the resultant moment on the top plate, $\boldsymbol{n_S} = \boldsymbol{W}'_{Am}\boldsymbol{T_S}$ is the moment from the sum of the sets of two wire tensions of the DAMs, and $\boldsymbol{n_D} = \boldsymbol{W}_{Cnz}\boldsymbol{T_D}$ is the moment from the difference of the sets of two wire tensions of the DAMs. Matrix $\boldsymbol{W}'_{Am}$ is the part of matrix $\boldsymbol{W}'_A$ related to the resultant moment while matrix $\boldsymbol{W}_{Cnz}$ is the non-zero part of matrix $\boldsymbol{W}_C$.

Figure 6 shows the vector form of Eq. (25). Theoretically, because $\boldsymbol{n_S}$ always has a positive value and $\boldsymbol{n_D}$ has much smaller value than $\boldsymbol{n_S}$, $\boldsymbol{n}$ always has a positive value and can be produced in any direction. To check the ability for producing force in any direction, the moment $\boldsymbol{n_S}$ will be used; however, to produce global motion, the resultant moment $\boldsymbol{n}$ needs to be in any direction.

To check whether a conventional wire mechanism can produce force in any direction, the force closure condition is used for workspace analysis [20, 21]. On the other hand, the vector closure condition is discussed in [1, 22] as a simpler way to evaluate the ability to produce force in any direction of conventional wire mechanism. For

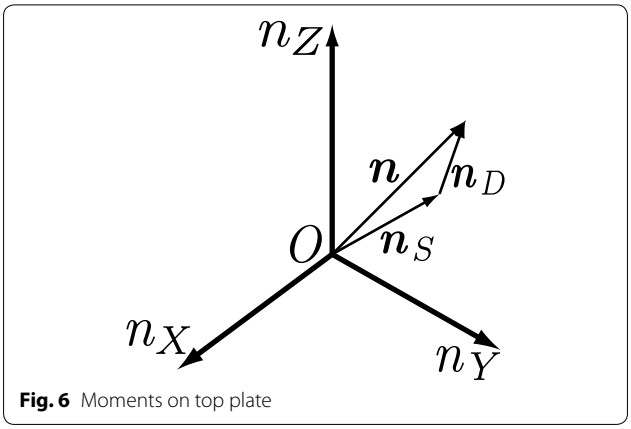

Fig. 6 Moments on top plate

developing RDWM, the modified vector closure condition is expressed as follows:

In an n-dimension space, an RDWM with N DAMs ($N \geq n+1$) *is said to satisfy the vector closure condition if the wire matrix of global motion* $\boldsymbol{W}'_A$ *satisfies the following two conditions:*

(C1) rank $(\boldsymbol{W}'_A) = n$.

(C2) There exists a vector $\boldsymbol{T_S} > \boldsymbol{0}$ that satisfies $\boldsymbol{W}'_A\boldsymbol{T_S} = \boldsymbol{0}$.

Any wire mechanism wherein matrix $\boldsymbol{W}'_A$ satisfies the two conditions (C1), (C2) will satisfy the vector closure condition and the resultant force can be produced in any direction in the motion space.

Numerical examples

Mechanisms do not satisfy vector closure condition

The mechanism does not satisfy the 1st point of vector closure condition

A planar RDWM does not satisfy the 1st point of vector closure condition is shown in Fig. 7. Here, the unit of the values of parameters related to length are assumed to be [cm]. The processes for deriving the matrix $\boldsymbol{W}'_{A2}$ and checking the vector closure condition are shown below:

Defining ${}^T\boldsymbol{p}_{TCi}$, R_i, ${}^T\boldsymbol{p}_{TDi}$ and ${}^T\boldsymbol{p}_{Bij}$

Select the parameters for the mechanism in Fig. 7 as follows:

$${}^T\boldsymbol{p}_{TC1} = [-6 \quad -10]^{\mathrm{T}}, \quad {}^T\boldsymbol{p}_{TC2} = [6 \quad -10]^{\mathrm{T}},$$
$${}^T\boldsymbol{p}_{TC3} = [6 \quad 10]^{\mathrm{T}}, \quad {}^T\boldsymbol{p}_{TC4} = [-6 \quad 10]^{\mathrm{T}}.$$

Radii of the pulleys: $R_1 = R_2 = R_3 = R_4 = 2$.

$${}^T\boldsymbol{p}_{TD1} = [-2 \quad 0]^{\mathrm{T}}, \quad {}^T\boldsymbol{p}_{TD2} = [-2 \quad 0]^{\mathrm{T}},$$
$${}^T\boldsymbol{p}_{TD3} = [2 \quad 0]^{\mathrm{T}}, \quad {}^T\boldsymbol{p}_{TD4} = [2 \quad 0]^{\mathrm{T}}.$$

Position of wire end points on the top plate w.r.t the top plate coordinate:

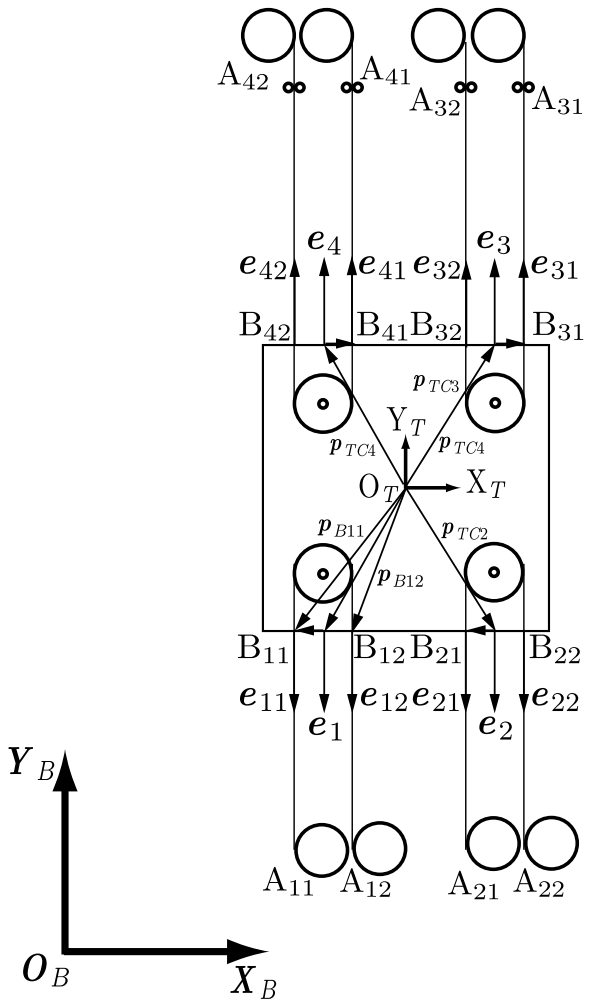

Fig. 7 The mechanism does not satisfy the 1st point of vector closure condition

$$
\begin{aligned}
{}^{T}\boldsymbol{p}_{B11} &= [-8 \quad -10]^{\mathrm{T}}, & {}^{T}\boldsymbol{p}_{B12} &= [-4 \quad -10]^{\mathrm{T}},\\
{}^{T}\boldsymbol{p}_{B21} &= [4 \quad -10]^{\mathrm{T}}, & {}^{T}\boldsymbol{p}_{B22} &= [8 \quad -10]^{\mathrm{T}},\\
{}^{T}\boldsymbol{p}_{B31} &= [8 \quad 10]^{\mathrm{T}}, & {}^{T}\boldsymbol{p}_{B32} &= [4 \quad 10]^{\mathrm{T}},\\
{}^{T}\boldsymbol{p}_{B41} &= [-4 \quad 10]^{\mathrm{T}}, & {}^{T}\boldsymbol{p}_{B42} &= [-8 \quad 10]^{\mathrm{T}}.
\end{aligned}
$$

Set of position ${}^{B}p_T$ and orientation ${}^{B}R_T$ of the top plate

$$
{}^{B}\boldsymbol{p}_{T} = [50 \quad 50]^{\mathrm{T}}, \quad {}^{B}\boldsymbol{R}_{T} = \begin{bmatrix} 1 & 0 \\ 0 & 1 \end{bmatrix}. \tag{26}
$$

Position of wire end points on the top plate

From Eq. (10), we have:

$$
\begin{aligned}
{}^{B}\boldsymbol{p}_{B11} &= [42 \quad 40]^{\mathrm{T}}, & {}^{B}\boldsymbol{p}_{B12} &= [46 \quad 40]^{\mathrm{T}},\\
{}^{B}\boldsymbol{p}_{B21} &= [54 \quad 40]^{\mathrm{T}}, & {}^{B}\boldsymbol{p}_{B22} &= [58 \quad 40]^{\mathrm{T}},\\
{}^{B}\boldsymbol{p}_{B31} &= [58 \quad 60]^{\mathrm{T}}, & {}^{B}\boldsymbol{p}_{B32} &= [54 \quad 60]^{\mathrm{T}},\\
{}^{B}\boldsymbol{p}_{B41} &= [46 \quad 60]^{\mathrm{T}}, & {}^{B}\boldsymbol{p}_{B42} &= [42 \quad 60]^{\mathrm{T}}.
\end{aligned}
$$

Position of wire end points on the frame

The DAMs are arranged on the frame such that the positions of the wire end points on the frame are as below:

$$
\begin{aligned}
{}^{B}\boldsymbol{p}_{A11} &= [42 \quad 20]^{\mathrm{T}}, & {}^{B}\boldsymbol{p}_{A12} &= [46 \quad 20]^{\mathrm{T}},\\
{}^{B}\boldsymbol{p}_{A21} &= [54 \quad 20]^{\mathrm{T}}, & {}^{B}\boldsymbol{p}_{A22} &= [58 \quad 20]^{\mathrm{T}},\\
{}^{B}\boldsymbol{p}_{A31} &= [58 \quad 90]^{\mathrm{T}}, & {}^{B}\boldsymbol{p}_{A32} &= [54 \quad 90]^{\mathrm{T}},\\
{}^{B}\boldsymbol{p}_{A41} &= [46 \quad 90]^{\mathrm{T}}, & {}^{B}\boldsymbol{p}_{A42} &= [42 \quad 90]^{\mathrm{T}}.
\end{aligned}
$$

Calculating the wire vectors ${}^{B}e_{ij}$

The wire vectors ${}^{B}\boldsymbol{e}_{ij}$ can be calculated using Eq. (11), and the results are shown below:

$$
\begin{aligned}
{}^{B}\boldsymbol{e}_{11} &= {}^{B}\boldsymbol{e}_{12} = {}^{B}\boldsymbol{e}_{21} = {}^{B}\boldsymbol{e}_{22} = [0 \quad -1]^{\mathrm{T}},\\
{}^{B}\boldsymbol{e}_{31} &= {}^{B}\boldsymbol{e}_{32} = {}^{B}\boldsymbol{e}_{41} = {}^{B}\boldsymbol{e}_{42} = [0 \quad 1]^{\mathrm{T}}.
\end{aligned}
$$

Checking if the two wires in the DAMs are in parallel

With this configuration, the two wires in the DAMs are in parallel.

Derivation of the matrix W'_{A2}

From Eqs. (6) and (16) with $n = 3$, $N = 4$, it is easy to see that the matrices $\boldsymbol{W}_2$ and $\boldsymbol{W}'_2$ have size 7×8. As mentioned in the previous section, both of them will not be used in the proposed judgment method. Therefore they are not necessary to be derived, only the matrix $\boldsymbol{W}'_{A2}$ will be used for the judgment and it is derived as follows:

From Eq. (12), the vectors ${}^{B}\boldsymbol{e}_i$ can be derived as:

$$
\begin{aligned}
{}^{B}\boldsymbol{e}_1 &= {}^{B}\boldsymbol{e}_2 = [0 \quad -1]^{\mathrm{T}},\\
{}^{B}\boldsymbol{e}_3 &= {}^{B}\boldsymbol{e}_4 = [0 \quad 1]^{\mathrm{T}},
\end{aligned}
$$

From Eq. (13), the vectors ${}^{B}\boldsymbol{p}_{TCi}$ can be derived as:

$$
\begin{aligned}
{}^{B}\boldsymbol{p}_{TC1} &= [44 \quad 40]^{\mathrm{T}}, & {}^{B}\boldsymbol{p}_{TC2} &= [56 \quad 40]^{\mathrm{T}},\\
{}^{B}\boldsymbol{p}_{TC3} &= [56 \quad 60]^{\mathrm{T}}, & {}^{B}\boldsymbol{p}_{TC4} &= [44 \quad 60]^{\mathrm{T}}.
\end{aligned}
$$

Then the wire matrix $\boldsymbol{W}'_{A2}$ from Eq. (17) becomes:

$$
\boldsymbol{W}'_{A2} = \begin{bmatrix} 0 & 0 & 0 & 0 \\ -1 & -1 & 1 & 1 \\ 6 & -6 & 6 & -6 \end{bmatrix}_{3\times 4}, \tag{27}
$$

The matrix $\boldsymbol{W}'_{A2}$ has size 3×4, with the row is equal to the number of DOFs in the planar global motion space and the column given by the four DOFs in the local motion space. It is about a quarter of the size of the wire matrix $\boldsymbol{W}_2$.

Vector closure condition check

Easily to see in this case that rank $(\boldsymbol{W}'_{A2}) = 2$, it is smaller than the number of dimension space of this wire mechanism (=3). Therefore, this mechanism can only realize the motion in two dimensions and it cannot realize motion in the remaining one. The first row of $\boldsymbol{W}'_{A2}$

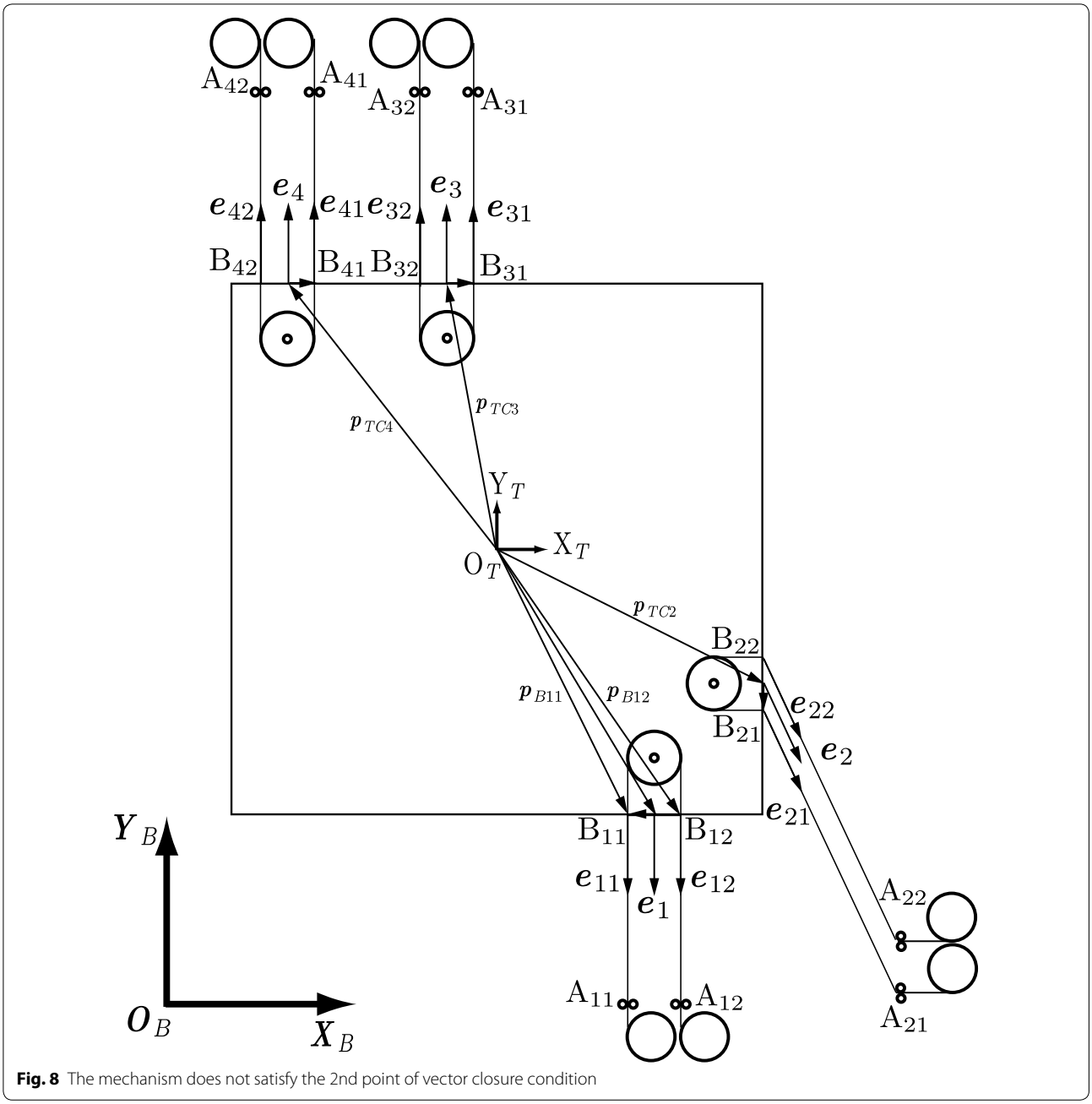

Fig. 8 The mechanism does not satisfy the 2nd point of vector closure condition

corresponds to the resultant force in X direction, and all the elements of the row are zero, which causes the rank ($\boldsymbol{W}'_{A2}$) to reduce one. The resultant force in X direction is zero so the motion in X direction can not be realized. This mechanism does not satisfy the 1st point which also means it does not satisfy vector closure condition.

The mechanism does not satisfy the 2nd point of vector closure condition

A planar RDWM does not satisfy the 2nd point of vector closure condition is shown in Fig. 8. Here, the unit of the values of parameters related to length are also assumed to be [cm]. The processes for deriving the matrix $\boldsymbol{W}'_{A2}$ and checking the vector closure condition are shown below:

Defining ${}^T\boldsymbol{p}_{TCi}$, $\boldsymbol{R}_i$, ${}^T\boldsymbol{p}_{TDi}$ and ${}^T\boldsymbol{p}_{Bij}$

Select the parameters for the mechanism in Fig. 8 as follows:

$$
{}^T\boldsymbol{p}_{TC1} = [16 \quad -20]^{\mathrm{T}}, \quad {}^T\boldsymbol{p}_{TC2} = [20 \quad -10]^{\mathrm{T}},
$$
$$
{}^T\boldsymbol{p}_{TC3} = [-4 \quad 20]^{\mathrm{T}}, \quad {}^T\boldsymbol{p}_{TC4} = [-16 \quad 20]^{\mathrm{T}}.
$$

Radii of the pulleys: $R_1 = R_2 = R_3 = R_4 = 2$.

$$^{T}\boldsymbol{p}_{TD1} = [-2 \quad 0]^{\mathrm{T}}, \quad ^{T}\boldsymbol{p}_{TD2} = [0 \quad -2]^{\mathrm{T}},$$
$$^{T}\boldsymbol{p}_{TD3} = [2 \quad 0]^{\mathrm{T}}, \quad ^{T}\boldsymbol{p}_{TD4} = [2 \quad 0]^{\mathrm{T}}.$$

Position of wire end points on the top plate w.r.t the top plate coordinate:

$$^{T}\boldsymbol{p}_{B11} = [14 \quad -20]^{\mathrm{T}}, \quad ^{T}\boldsymbol{p}_{B12} = [18 \quad -20]^{\mathrm{T}},$$
$$^{T}\boldsymbol{p}_{B21} = [20 \quad -12]^{\mathrm{T}}, \quad ^{T}\boldsymbol{p}_{B22} = [20 \quad -8]^{\mathrm{T}},$$
$$^{T}\boldsymbol{p}_{B31} = [-2 \quad 20]^{\mathrm{T}}, \quad ^{T}\boldsymbol{p}_{B32} = [-6 \quad 20]^{\mathrm{T}},$$
$$^{T}\boldsymbol{p}_{B41} = [-14 \quad 20]^{\mathrm{T}}, \quad ^{T}\boldsymbol{p}_{B42} = [-18 \quad 20]^{\mathrm{T}}.$$

Set of position $^{B}p_{T}$ and orientation $^{B}R_{T}$ of the top plate

$$^{B}\boldsymbol{p}_{T} = [50 \quad 50]^{\mathrm{T}}, \quad ^{B}\boldsymbol{R}_{T} = \begin{bmatrix} 1 & 0 \\ 0 & 1 \end{bmatrix}. \tag{28}$$

Position of wire end points on the top plate

From Eq. (10), we have:

$$^{B}\boldsymbol{p}_{B11} = [64 \quad 30]^{\mathrm{T}}, \quad ^{B}\boldsymbol{p}_{B12} = [68 \quad 30]^{\mathrm{T}},$$
$$^{B}\boldsymbol{p}_{B21} = [70 \quad 38]^{\mathrm{T}}, \quad ^{B}\boldsymbol{p}_{B22} = [70 \quad 42]^{\mathrm{T}},$$
$$^{B}\boldsymbol{p}_{B31} = [48 \quad 70]^{\mathrm{T}}, \quad ^{B}\boldsymbol{p}_{B32} = [44 \quad 70]^{\mathrm{T}},$$
$$^{B}\boldsymbol{p}_{B41} = [36 \quad 70]^{\mathrm{T}}, \quad ^{B}\boldsymbol{p}_{B42} = [32 \quad 70]^{\mathrm{T}}.$$

Position of wire end points on the frame

The DAMs are arranged on the frame such that the positions of the wire end points on the frame are as below:

$$^{B}\boldsymbol{p}_{A11} = [64 \quad 0]^{\mathrm{T}}, \quad ^{B}\boldsymbol{p}_{A12} = [68 \quad 0]^{\mathrm{T}},$$
$$^{B}\boldsymbol{p}_{A21} = [118 \quad 2]^{\mathrm{T}}, \quad ^{B}\boldsymbol{p}_{A22} = [118 \quad 6]^{\mathrm{T}},$$
$$^{B}\boldsymbol{p}_{A31} = [48 \quad 100]^{\mathrm{T}}, \quad ^{B}\boldsymbol{p}_{A32} = [44 \quad 100]^{\mathrm{T}},$$
$$^{B}\boldsymbol{p}_{A41} = [36 \quad 100]^{\mathrm{T}}, \quad ^{B}\boldsymbol{p}_{A42} = [32 \quad 100]^{\mathrm{T}}.$$

Calculating the wire vectors $^{B}e_{ij}$

The wire vectors $^{B}\boldsymbol{e}_{ij}$ can be calculated using Eq. (11), and the results are shown below:

$$^{B}\boldsymbol{e}_{11} = {}^{B}\boldsymbol{e}_{12} = [0 \quad -1]^{\mathrm{T}}, \; ^{B}\boldsymbol{e}_{21} = {}^{B}\boldsymbol{e}_{22} = [4/5 \quad -3/5]^{\mathrm{T}},$$
$$^{B}\boldsymbol{e}_{31} = {}^{B}\boldsymbol{e}_{32} = {}^{B}\boldsymbol{e}_{41} = {}^{B}\boldsymbol{e}_{42} = [0 \quad 1]^{\mathrm{T}}.$$

Checking if the two wires in the DAMs are in parallel

With this configuration, the two wires in the DAMs are in parallel.

Derivation of the matrix W'_{A2}

From Eqs. (6) and (16) with $n = 3$, $N = 4$, it is easy to see that the matrices $\boldsymbol{W}_2$ and $\boldsymbol{W}'_2$ have size 7×8. Similarly to the previous example, these matrices are not necessary to be derived, only the matrix $\boldsymbol{W}'_{A2}$ will be used for the judgment and it is derived as follows:

From Eq. (12), the vectors $^{B}\boldsymbol{e}_i$ can be derived as:

$$^{B}\boldsymbol{e}_1 = [0 \quad -1]^{\mathrm{T}}, \; ^{B}\boldsymbol{e}_2 = [4/5 \quad -3/5]^{\mathrm{T}}, \; ^{B}\boldsymbol{e}_3 = {}^{B}\boldsymbol{e}_4 = [0 \quad 1]^{\mathrm{T}}.$$

From Eq. (13), the vectors $^{B}\boldsymbol{p}_{TCi}$ can be derived as:

$$^{B}\boldsymbol{p}_{TC1} = [66 \quad 30]^{\mathrm{T}}, \quad ^{B}\boldsymbol{p}_{TC2} = [70 \quad 40]^{\mathrm{T}},$$
$$^{B}\boldsymbol{p}_{TC3} = [46 \quad 70]^{\mathrm{T}}, \quad ^{B}\boldsymbol{p}_{TC4} = [34 \quad 70]^{\mathrm{T}}.$$

Then the wire matrix $\boldsymbol{W}'_{A2}$ from Eq. (17) becomes:

$$\boldsymbol{W}'_{A2} = \begin{bmatrix} 0 & 4/5 & 0 & 0 \\ -1 & -3/5 & 1 & 1 \\ -16 & -4 & -4 & -16 \end{bmatrix}_{3\times 4}, \tag{29}$$

Similarly to the previous example, the matrix $\boldsymbol{W}'_{A2}$ related to the global motion in this case also equals just a quarter of the normal wire matrix $\boldsymbol{W}_2$.

Vector closure condition check

Easily to see in this case that rank $(\boldsymbol{W}'_{A2}) = 3$. It equals to the number of dimension space of the wire mechanism (=3) so it satisfies the 1st point of vector closure condition. However considering the 3rd row of $\boldsymbol{W}'_{A2}$, this row corresponds to the resultant moment. It has all elements with negative values so with any positive wire tension $\boldsymbol{T}_0$, the resultant moment will be produced only negative value. Therefore no wire tension $\boldsymbol{T}_0$ satisfies $\boldsymbol{W}'_{A2}\boldsymbol{T}_0 = 0$. This mechanism does not satisfy the 2nd point which also means it does not satisfy vector closure condition.

Mechanisms satisfy vector closure condition

The planar RDWM with DAMs

A planar RDWM with DAMs is shown in Fig. 9. Here, the unit of the values of parameters related to length are assumed to be [cm]. The processes for deriving the matrix $\boldsymbol{W}'_{A2}$ and checking the vector closure condition are shown below:

Defining $^{T}p_{TCi}$, R_i, $^{T}p_{TDi}$ and $^{T}p_{Bij}$

Select the parameters for the mechanism in Fig. 9 as follows:

$$^{T}\boldsymbol{p}_{TC1} = [-6 \quad 10]^{\mathrm{T}}, \quad ^{T}\boldsymbol{p}_{TC2} = [-10 \quad -6]^{\mathrm{T}},$$
$$^{T}\boldsymbol{p}_{TC3} = [10 \quad -6]^{\mathrm{T}}, \quad ^{T}\boldsymbol{p}_{TC4} = [6 \quad 10]^{\mathrm{T}}.$$

Radii of the pulleys: $R_1 = R_2 = R_3 = R_4 = 2$.

$$^{T}\boldsymbol{p}_{TD1} = [2 \quad 0]^{\mathrm{T}}, \quad ^{T}\boldsymbol{p}_{TD2} = [0 \quad 2]^{\mathrm{T}},$$
$$^{T}\boldsymbol{p}_{TD3} = [0 \quad -2]^{\mathrm{T}}, \quad ^{T}\boldsymbol{p}_{TD4} = [2 \quad 0]^{\mathrm{T}}.$$

Position of wire end points on the top plate w.r.t the top plate coordinate:

$$^{T}\boldsymbol{p}_{B11} = [-4 \quad 10]^{\mathrm{T}}, \quad ^{T}\boldsymbol{p}_{B12} = [-8 \quad 10]^{\mathrm{T}},$$
$$^{T}\boldsymbol{p}_{B21} = [-10 \quad -4]^{\mathrm{T}}, \quad ^{T}\boldsymbol{p}_{B22} = [-10 \quad -8]^{\mathrm{T}},$$
$$^{T}\boldsymbol{p}_{B31} = [10 \quad -8]^{\mathrm{T}}, \quad ^{T}\boldsymbol{p}_{B32} = [10 \quad -4]^{\mathrm{T}},$$
$$^{T}\boldsymbol{p}_{B41} = [8 \quad 10]^{\mathrm{T}}, \quad ^{T}\boldsymbol{p}_{B42} = [4 \quad 10]^{\mathrm{T}}.$$

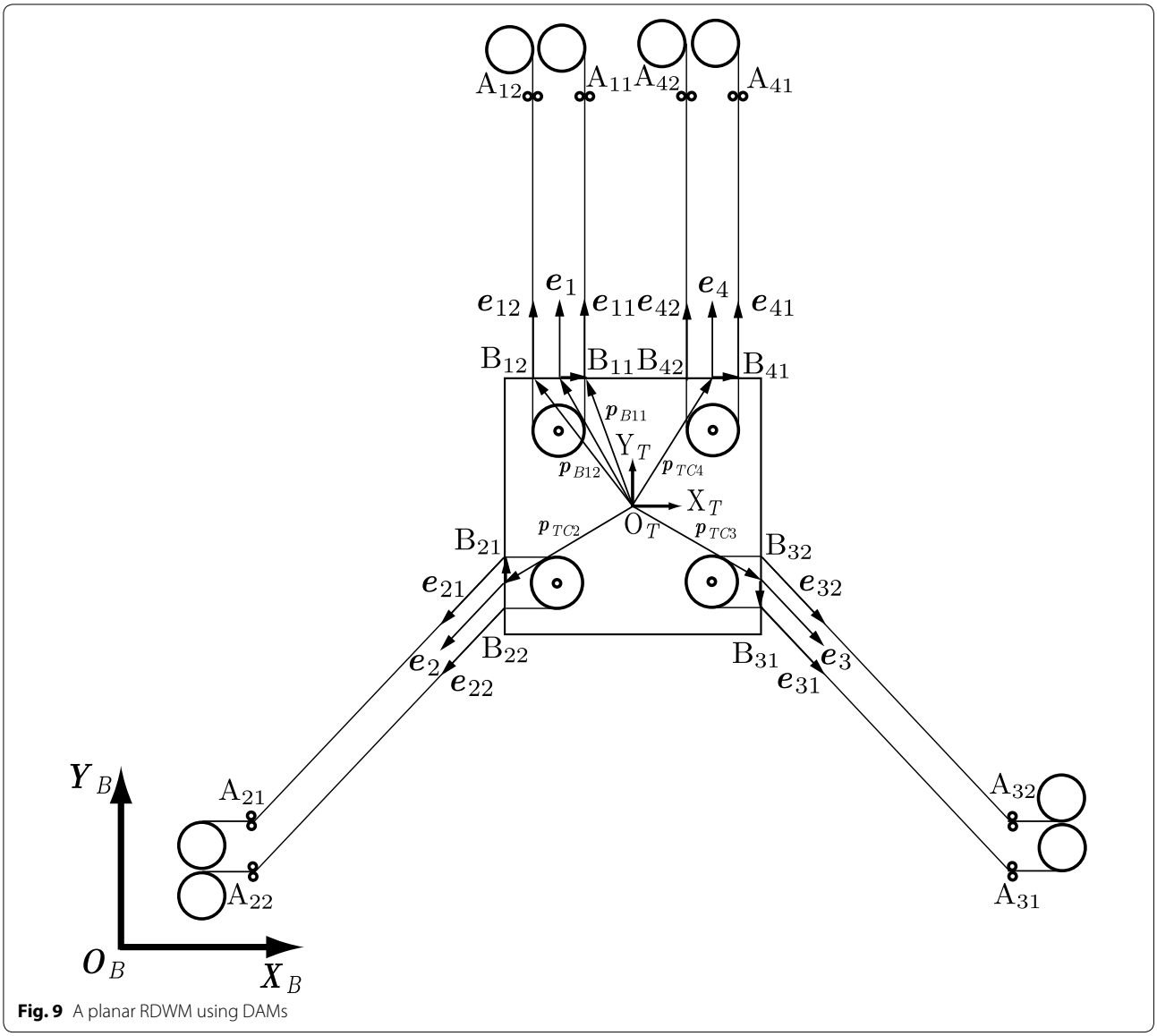

Fig. 9 A planar RDWM using DAMs

Set of position ${}^B p_T$ and orientation ${}^B R_T$ of the top plate

$$ {}^B\boldsymbol{p}_T = [50 \quad 50]^{\mathrm{T}}, \quad {}^B\boldsymbol{R}_T = \begin{bmatrix} 1 & 0 \\ 0 & 1 \end{bmatrix}. \tag{30} $$

Position of wire end points on the top plate

From Eq. (10), we have:

$$ \begin{aligned} {}^B\boldsymbol{p}_{B11} &= [46 \quad 60]^{\mathrm{T}}, & {}^B\boldsymbol{p}_{B12} &= [42 \quad 60]^{\mathrm{T}}, \\ {}^B\boldsymbol{p}_{B21} &= [40 \quad 46]^{\mathrm{T}}, & {}^B\boldsymbol{p}_{B22} &= [40 \quad 42]^{\mathrm{T}}, \\ {}^B\boldsymbol{p}_{B31} &= [60 \quad 42]^{\mathrm{T}}, & {}^B\boldsymbol{p}_{B32} &= [60 \quad 46]^{\mathrm{T}}, \\ {}^B\boldsymbol{p}_{B41} &= [58 \quad 60]^{\mathrm{T}}, & {}^B\boldsymbol{p}_{B42} &= [54 \quad 60]^{\mathrm{T}}. \end{aligned} $$

Position of wire end points on the frame

The DAMs are arranged on the frame such that the positions of the wire end points on the frame are as below:

$$ \begin{aligned} {}^B\boldsymbol{p}_{A11} &= [46 \quad 90]^{\mathrm{T}}, & {}^B\boldsymbol{p}_{A12} &= [42 \quad 90]^{\mathrm{T}}, \\ {}^B\boldsymbol{p}_{A21} &= [10 \quad 23.5]^{\mathrm{T}}, & {}^B\boldsymbol{p}_{A22} &= [10 \quad 19.5]^{\mathrm{T}}, \\ {}^B\boldsymbol{p}_{A31} &= [90 \quad 19.5]^{\mathrm{T}}, & {}^B\boldsymbol{p}_{A32} &= [90 \quad 23.5]^{\mathrm{T}}, \\ {}^B\boldsymbol{p}_{A41} &= [58 \quad 90]^{\mathrm{T}}, & {}^B\boldsymbol{p}_{A42} &= [54 \quad 90]^{\mathrm{T}}. \end{aligned} $$

Calculating the wire vectors ${}^B e_{ij}$

The wire vectors ${}^B\boldsymbol{e}_{ij}$ can be calculated using Eq. (11), and the results are shown below:

$$ \begin{aligned} {}^B\boldsymbol{e}_{11} &= {}^B\boldsymbol{e}_{12} = [0 \quad 1]^{\mathrm{T}}, \\ {}^B\boldsymbol{e}_{21} &= {}^B\boldsymbol{e}_{22} = [-4/5 \quad -3/5]^{\mathrm{T}}, \\ {}^B\boldsymbol{e}_{31} &= {}^B\boldsymbol{e}_{32} = [4/5 \quad -3/5]^{\mathrm{T}}, \\ {}^B\boldsymbol{e}_{41} &= {}^B\boldsymbol{e}_{42} = [0 \quad 1]^{\mathrm{T}}. \end{aligned} $$

Checking if the two wires in the DAMs are in parallel

With this configuration, the two wires in the DAMs are in parallel.

Derivation of the matrix $W_A^{'}$

From Eqs. (6) and (16) with $n = 3$, $N = 4$, it is easy to see that the matrices $\boldsymbol{W}_2$ and $\boldsymbol{W}_2^{'}$ have size 7×8. Similarly to the previous examples, these matrices are not necessary to be derived, only the matrix $\boldsymbol{W}_{A2}^{'}$ will be used for the judgment and it is derived as follows:

From Eq. (12), the vectors ${}^{B}\boldsymbol{e}_i$ can be derived as:

$$\begin{aligned} {}^{B}\boldsymbol{e}_1 &= [0 \quad 1]^{\mathrm{T}}, \quad {}^{B}\boldsymbol{e}_2 = [-4/5 \quad -3/5]^{\mathrm{T}}, \\ {}^{B}\boldsymbol{e}_3 &= [4/5 \quad -3/5]^{\mathrm{T}}, \quad {}^{B}\boldsymbol{e}_4 = [0 \quad 1]^{\mathrm{T}} \end{aligned}$$

From Eq. (13), the vectors ${}^{B}\boldsymbol{p}_{TCi}$ can be derived as:

$$\begin{aligned} {}^{B}\boldsymbol{p}_{TC1} &= [44 \quad 60]^{\mathrm{T}}, \quad {}^{B}\boldsymbol{p}_{TC2} = [40 \quad 44]^{\mathrm{T}}, \\ {}^{B}\boldsymbol{p}_{TC3} &= [60 \quad 44]^{\mathrm{T}}, \quad {}^{B}\boldsymbol{p}_{TC4} = [56 \quad 60]^{\mathrm{T}}. \end{aligned}$$

Then the matrix $\boldsymbol{W}_{A2}^{'}$ from Eq. (17) becomes:

$$\boldsymbol{W}_{A2}^{'} = \begin{bmatrix} 0 & -\frac{4}{5} & \frac{4}{5} & 0 \\ 1 & -\frac{3}{5} & -\frac{3}{5} & 1 \\ -6 & \frac{6}{5} & -\frac{6}{5} & 6 \end{bmatrix}_{3\times 4}, \tag{31}$$

Similarly to the previous examples, the matrix $\boldsymbol{W}_{A2}^{'}$ related to the global motion in this case also equals just a quarter of the normal wire matrix $\boldsymbol{W}_2$.

Vector closure condition check

From the expression in the judgment of a candidate section, only the matrix that contributes to global motion $\boldsymbol{W}_{A2}^{'}$ is needed to check the vector closure condition. Using the matrix of global motion from Eq. (31), we have:

(i) rank $(\boldsymbol{W}_{A2}^{'}) = 3$.

(ii) With $\boldsymbol{T}_{S2} = \begin{bmatrix} 3 & 5 & 5 & 3 \end{bmatrix}^{\mathrm{T}} > \boldsymbol{0}$, easy to get $\boldsymbol{W}_{A2}^{'}\boldsymbol{T}_{S2} = \boldsymbol{0}$.

The above analysis shows that rank $(\boldsymbol{W}_{A2}^{'})$ equals to the number of dimension spaces of the wire mechanism. As there is a vector $\boldsymbol{T}_{S2}$ that satisfies $\boldsymbol{W}_{A2}^{'}\boldsymbol{T}_{S2} = \boldsymbol{0}$, the matrix $\boldsymbol{W}_{A2}^{'}$ satisfies the vector closure condition and the mechanism can produce the resultant force in any direction within its motion space. The results mean that the planar RDWM with four sets of DAMs in this example has the same structure as that of a conventional wire mechanism with four sets of single actuator modules, where each wire is equivalent to a set of two wires for each DAM in the planar RDWM, when judging the vector closure condition.

The 3D RDWM with DAMs

A 3D RDWM with DAMs is shown in Fig. 10. Here, the unit of the values of parameters related to length are assumed to be [cm]. Because of space limitations, the DAMs are not shown; only the end points of the wires on those modules are shown, with the important representative vectors. The processes for deriving the matrix $\boldsymbol{W}_{A3}^{'}$ and checking the vector closure condition are shown below:

Defining ${}^{T}\boldsymbol{p}_{TCi}$, $\boldsymbol{R}_i$, ${}^{T}\boldsymbol{p}_{TDi}$, and ${}^{T}\boldsymbol{p}_{Bij}$

Select the parameters for the mechanism in Fig. 10 as follows:

$$\begin{aligned} {}^{T}\boldsymbol{p}_{TC1} &= [-6 \quad 10 \quad 10]^{\mathrm{T}}, & {}^{T}\boldsymbol{p}_{TC2} &= [-10 \quad -6 \quad 10]^{\mathrm{T}}, \\ {}^{T}\boldsymbol{p}_{TC3} &= [10 \quad -6 \quad 10]^{\mathrm{T}}, & {}^{T}\boldsymbol{p}_{TC4} &= [6 \quad 10 \quad 10]^{\mathrm{T}}, \\ {}^{T}\boldsymbol{p}_{TC5} &= [-10 \quad 6 \quad -10]^{\mathrm{T}}, & {}^{T}\boldsymbol{p}_{TC6} &= [0 \quad -10 \quad -10]^{\mathrm{T}}, \\ {}^{T}\boldsymbol{p}_{TC7} &= [10 \quad 6 \quad -10]^{\mathrm{T}}. \end{aligned}$$

Radii of the pulleys: $R_1 = R_2 = R_3 = R_4 = R_5 = R_6 = R_7 = 2$.

$$\begin{aligned} {}^{T}\boldsymbol{p}_{TD1} &= [2 \quad 0 \quad 0]^{\mathrm{T}}, & {}^{T}\boldsymbol{p}_{TD2} &= [0 \quad 2 \quad 0]^{\mathrm{T}}, \\ {}^{T}\boldsymbol{p}_{TD3} &= [0 \quad -2 \quad 0]^{\mathrm{T}}, & {}^{T}\boldsymbol{p}_{TD4} &= [2 \quad 0 \quad 0]^{\mathrm{T}}, \\ {}^{T}\boldsymbol{p}_{TD5} &= [0 \quad 2 \quad 0]^{\mathrm{T}}, & {}^{T}\boldsymbol{p}_{TD6} &= [-2 \quad 0 \quad 0]^{\mathrm{T}}, \\ {}^{T}\boldsymbol{p}_{TD7} &= [0 \quad -2 \quad 0]^{\mathrm{T}}. \end{aligned}$$

The positions of wire end points on the top plate w.r.t the top plate coordinate are given by:

$$\begin{aligned} {}^{T}\boldsymbol{p}_{B11} &= [-4 \quad 10 \quad 10]^{\mathrm{T}}, & {}^{T}\boldsymbol{p}_{B12} &= [-8 \quad 10 \quad 10]^{\mathrm{T}}, \\ {}^{T}\boldsymbol{p}_{B21} &= [-10 \quad -4 \quad 10]^{\mathrm{T}}, & {}^{T}\boldsymbol{p}_{B22} &= [-10 \quad -8 \quad 10]^{\mathrm{T}}, \\ {}^{T}\boldsymbol{p}_{B31} &= [10 \quad -8 \quad 10]^{\mathrm{T}}, & {}^{T}\boldsymbol{p}_{B32} &= [10 \quad -4 \quad 10]^{\mathrm{T}}, \\ {}^{T}\boldsymbol{p}_{B41} &= [8 \quad 10 \quad 10]^{\mathrm{T}}, & {}^{T}\boldsymbol{p}_{B42} &= [4 \quad 10 \quad 10]^{\mathrm{T}}, \\ {}^{T}\boldsymbol{p}_{B51} &= [-10 \quad 8 \quad -10]^{\mathrm{T}}, & {}^{T}\boldsymbol{p}_{B52} &= [-10 \quad 4 \quad -10]^{\mathrm{T}}, \\ {}^{T}\boldsymbol{p}_{B61} &= [-2 \quad -10 \quad -10]^{\mathrm{T}}, & {}^{T}\boldsymbol{p}_{B62} &= [2 \quad -10 \quad -10]^{\mathrm{T}}, \\ {}^{T}\boldsymbol{p}_{B71} &= [10 \quad 4 \quad -10]^{\mathrm{T}}, & {}^{T}\boldsymbol{p}_{B72} &= [10 \quad 8 \quad -10]^{\mathrm{T}}. \end{aligned}$$

Set of position ${}^{B}\boldsymbol{p}_T$ and orientation ${}^{B}\boldsymbol{R}_T$ of the top plate

$${}^{B}\boldsymbol{p}_T = [50 \quad 50 \quad 50]^{\mathrm{T}}, \quad {}^{B}\boldsymbol{R}_T = \begin{bmatrix} 1 & 0 & 0 \\ 0 & 1 & 0 \\ 0 & 0 & 1 \end{bmatrix}. \tag{32}$$

Position of wire end points on the top plate

From Eq. (10), we have:

$$\begin{aligned} {}^{B}\boldsymbol{p}_{B11} &= [46 \quad 60 \quad 60]^{\mathrm{T}}, & {}^{B}\boldsymbol{p}_{B12} &= [42 \quad 60 \quad 60]^{\mathrm{T}}, \\ {}^{B}\boldsymbol{p}_{B21} &= [40 \quad 46 \quad 60]^{\mathrm{T}}, & {}^{B}\boldsymbol{p}_{B22} &= [40 \quad 42 \quad 60]^{\mathrm{T}}, \\ {}^{B}\boldsymbol{p}_{B31} &= [60 \quad 42 \quad 60]^{\mathrm{T}}, & {}^{B}\boldsymbol{p}_{B32} &= [60 \quad 46 \quad 60]^{\mathrm{T}}, \\ {}^{B}\boldsymbol{p}_{B41} &= [58 \quad 60 \quad 60]^{\mathrm{T}}, & {}^{B}\boldsymbol{p}_{B42} &= [54 \quad 60 \quad 60]^{\mathrm{T}}, \\ {}^{B}\boldsymbol{p}_{B51} &= [40 \quad 58 \quad 40]^{\mathrm{T}}, & {}^{B}\boldsymbol{p}_{B52} &= [40 \quad 54 \quad 40]^{\mathrm{T}}, \\ {}^{B}\boldsymbol{p}_{B61} &= [48 \quad 40 \quad 40]^{\mathrm{T}}, & {}^{B}\boldsymbol{p}_{B62} &= [52 \quad 10 \quad 40]^{\mathrm{T}}, \\ {}^{B}\boldsymbol{p}_{B71} &= [60 \quad 54 \quad 40]^{\mathrm{T}}, & {}^{B}\boldsymbol{p}_{B72} &= [60 \quad 58 \quad 40]^{\mathrm{T}}. \end{aligned}$$

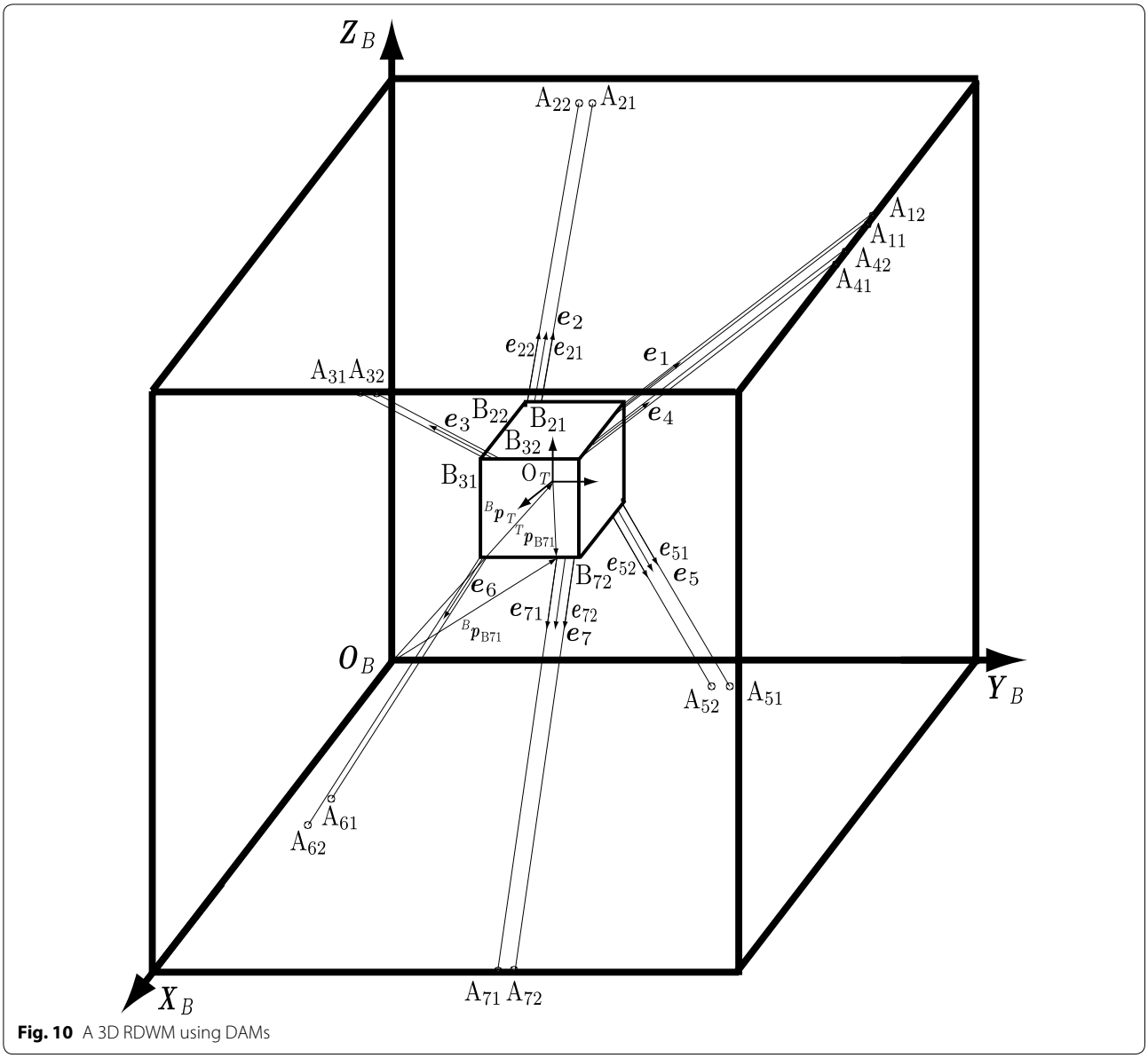

Fig. 10 A 3D RDWM using DAMs

Position of wire end points on the frame

The DAMs are arranged on the frame such that the positions of the wire end points on the frame are as shown below:

$$
\begin{aligned}
{}^B\boldsymbol{p}_{A11} &= [46 \quad 90 \quad 100]^{\mathrm{T}}, & {}^B\boldsymbol{p}_{A12} &= [42 \quad 90 \quad 100]^{\mathrm{T}},\\
{}^B\boldsymbol{p}_{A21} &= [10 \quad 46 \quad 100]^{\mathrm{T}}, & {}^B\boldsymbol{p}_{A22} &= [10 \quad 42 \quad 100]^{\mathrm{T}},\\
{}^B\boldsymbol{p}_{A31} &= [90 \quad 42 \quad 100]^{\mathrm{T}}, & {}^B\boldsymbol{p}_{A32} &= [90 \quad 46 \quad 100]^{\mathrm{T}},\\
{}^B\boldsymbol{p}_{A41} &= [58 \quad 90 \quad 100]^{\mathrm{T}}, & {}^B\boldsymbol{p}_{A42} &= [54 \quad 90 \quad 100]^{\mathrm{T}},\\
{}^B\boldsymbol{p}_{A51} &= [10 \quad 58 \quad 0]^{\mathrm{T}}, & {}^B\boldsymbol{p}_{A52} &= [10 \quad 54 \quad 0]^{\mathrm{T}},\\
{}^B\boldsymbol{p}_{A61} &= [48 \quad 10 \quad 0]^{\mathrm{T}}, & {}^B\boldsymbol{p}_{A62} &= [52 \quad 10 \quad 0]^{\mathrm{T}},\\
{}^B\boldsymbol{p}_{A71} &= [90 \quad 54 \quad 0]^{\mathrm{T}}, & {}^B\boldsymbol{p}_{A72} &= [90 \quad 58 \quad 0]^{\mathrm{T}}.
\end{aligned}
$$

Calculating the wire vectors ${}^B\boldsymbol{e}_{ij}$

The wire vectors ${}^B\boldsymbol{e}_{ij}$ can be calculated using Eq. (11), and the results are shown below:

$$
\begin{aligned}
{}^B\boldsymbol{e}_{11} &= {}^B\boldsymbol{e}_{12} = [0 \quad 3/5 \quad 4/5]^{\mathrm{T}},\\
{}^B\boldsymbol{e}_{21} &= {}^B\boldsymbol{e}_{22} = [-3/5 \quad 0 \quad 4/5]^{\mathrm{T}},\\
{}^B\boldsymbol{e}_{31} &= {}^B\boldsymbol{e}_{32} = [3/5 \quad 0 \quad 4/5]^{\mathrm{T}},\\
{}^B\boldsymbol{e}_{41} &= {}^B\boldsymbol{e}_{42} = [0 \quad 3/5 \quad 4/5]^{\mathrm{T}},\\
{}^B\boldsymbol{e}_{51} &= {}^B\boldsymbol{e}_{52} = [-3/5 \quad 0 \quad -4/5]^{\mathrm{T}},\\
{}^B\boldsymbol{e}_{61} &= {}^B\boldsymbol{e}_{62} = [0 \quad -3/5 \quad -4/5]^{\mathrm{T}},\\
{}^B\boldsymbol{e}_{71} &= {}^B\boldsymbol{e}_{72} = [3/5 \quad 0 \quad -4/5]^{\mathrm{T}}.
\end{aligned}
$$

Checking if the two wires in the DAMs are in parallel

With this configuration, the two wires in the DAMs are in parallel.

Derivation of the matrix $W_A^{'}$

From Eqs. (6) and (16) with $n = 6$, $N = 7$, it is easy to see that the matrices $\boldsymbol{W}_3$ and $\boldsymbol{W}_3^{'}$ have size 13×14. Similarly to the previous examples, these matrices are not necessary to be derived, only the matrix $\boldsymbol{W}_{A3}^{'}$ will be used for the judgment and it is derived as follows:

From Eq. (12), the vectors ${}^B\boldsymbol{e}_i$ can be derived as:

$$
\begin{aligned}
&{}^B\boldsymbol{e}_1 = [0 \quad 3/5 \quad 4/5]^{\mathrm{T}}, && {}^B\boldsymbol{e}_2 = [-3/5 \quad 0 \quad 4/5]^{\mathrm{T}},\\
&{}^B\boldsymbol{e}_3 = [3/5 \quad 0 \quad 4/5]^{\mathrm{T}}, && {}^B\boldsymbol{e}_4 = [0 \quad 3/5 \quad 4/5]^{\mathrm{T}},\\
&{}^B\boldsymbol{e}_5 = [-3/5 \quad 0 \quad -4/5]^{\mathrm{T}}, && {}^B\boldsymbol{e}_6 = [0 \quad -3/5 \quad -4/5]^{\mathrm{T}},\\
&{}^B\boldsymbol{e}_7 = [3/5 \quad 0 \quad -4/5]^{\mathrm{T}}.
\end{aligned}
$$

From Eq. (13), the vectors ${}^B\boldsymbol{p}_{TCi}$ can be derived as:

$$
\begin{aligned}
&{}^B\boldsymbol{p}_{TC1} = [44 \quad 60 \quad 60]^{\mathrm{T}}, && {}^B\boldsymbol{p}_{TC2} = [40 \quad 44 \quad 60]^{\mathrm{T}},\\
&{}^B\boldsymbol{p}_{TC3} = [60 \quad 44 \quad 60]^{\mathrm{T}}, && {}^B\boldsymbol{p}_{TC4} = [56 \quad 60 \quad 60]^{\mathrm{T}}.\\
&{}^B\boldsymbol{p}_{TC5} = [40 \quad 56 \quad 40]^{\mathrm{T}}, && {}^B\boldsymbol{p}_{TC6} = [50 \quad 25 \quad 40]^{\mathrm{T}},\\
&{}^B\boldsymbol{p}_{TC7} = [60 \quad 56 \quad 40]^{\mathrm{T}}.
\end{aligned}
$$

Then the matrix $\boldsymbol{W}_{A3}^{'}$ from Eq. (17) becomes:

$$
\boldsymbol{W}_{A3}^{'} = \begin{bmatrix}
0 & -\frac{3}{5} & \frac{3}{5} & 0 & -\frac{3}{5} & 0 & \frac{3}{5}\\
\frac{3}{5} & 0 & 0 & \frac{3}{5} & 0 & -\frac{3}{5} & 0\\
\frac{4}{5} & \frac{4}{5} & \frac{4}{5} & \frac{4}{5} & -\frac{4}{5} & -\frac{4}{5} & -\frac{4}{5}\\
2 & -\frac{24}{5} & -\frac{24}{5} & 2 & -\frac{24}{5} & 2 & -\frac{24}{5}\\
\frac{24}{5} & 2 & -2 & -\frac{24}{5} & -2 & 0 & 2\\
-\frac{18}{5} & -\frac{18}{5} & \frac{18}{5} & \frac{18}{5} & \frac{18}{5} & 0 & -\frac{18}{5}
\end{bmatrix}_{6\times 7}, \tag{33}
$$

The matrix $\boldsymbol{W}_{A3}^{'}$ has size 6×7, where the number of rows is equal to the six DOFs in the 3D global motion space and the number of columns is equal to the seven DOFs in the local motion space. It is about a quarter of the size of the wire matrix $\boldsymbol{W}_3$.

Vector closure condition check

From the expression in the judgment of a candidate section, only the matrix that contributes to global motion $\boldsymbol{W}_{A3}^{'}$ is needed to check the vector closure condition. Using the matrix of global motion from Eq. (33), we have:

(i) rank $(\boldsymbol{W}_{A3}^{'}) = 6$.
(ii) With $\boldsymbol{T}_{S3} = \begin{bmatrix} 12 & 5 & 5 & 12 & 5 & 24 & 5 \end{bmatrix}^{\mathrm{T}} > \boldsymbol{0}$, easy to get $\boldsymbol{W}_{A3}^{'}\boldsymbol{T}_{S3} = \boldsymbol{0}$.

The above analysis shows that rank $(\boldsymbol{W}_{A3}^{'})$ equals to the number of dimension spaces of the wire mechanism. As there is a vector $\boldsymbol{T}_{S3}$ that satisfies $\boldsymbol{W}_{A3}^{'}\boldsymbol{T}_{S3} = \boldsymbol{0}$, the matrix $\boldsymbol{W}_{A3}^{'}$ satisfies the vector closure condition and the mechanism can produce the resultant force in any direction within its motion space. The results mean that the 3D RDWM with seven sets of DAMs in this example has the same structure as a conventional wire mechanism with seven sets of single actuator modules, wherein each wire in the conventional wire mechanism is equivalent to a set of two wires of each DAM in the 3D RDWM, in judgment with the vector closure condition.

Remark

The above examples show the advantages of the proposed judgment method for RDWM's configurations. It specially shows the effects in the case of dealing with the multi-dimension mechanisms as the 3D case in the last example. In that case, we only have to deal with a 6×7 matrix instead of a 13×14 one. This will let the designers to focus on thinking about arranging the configurations and then they can check those configurations with faster, simpler and easier way.

Discussion: designing an RDWM

Constructing a local mechanism [15]

As an example of how to construct a local mechanism, a 1D RDWM with local motions is presented in Fig. 11. The top plate is controlled using two sets of DAMs. When the two actuators in a DAM rotate in the same direction, a translational motion of the top plate is produced. In contrast, when the two actuators rotate in different directions, local motions are produced on the top plate. Here, the local motions are utilized to produce the rotation of the two fingers when grasping and picking up an object. To allow the two fingers to perform fine motions, the gear ratio $N = Z_2/Z_1$ should be large.

Reducing the number of actuators [18]

When RDWM is extended to the 2D or 3D cases, the required number of actuators becomes large. The VCM can be used to reduce the number of actuators in the wire mechanism. As a consequence of using this module, the orientation of the top plate becomes fixed. An illustration of a wire mechanism using the VCM is shown in Fig. 12. The required number of actuators in this case is $\{(n-1)+1\} \times 2 = 6$ (where $n = 3$ is the number of DOFs in the 2D case). It requires only six units, reduced two units compared with the case where four DAMs, i.e. eight actuators, are used for producing high acceleration motion. In the same way, the required number of actuators is only eight in the 3D case. It reduces six units, compared with the case where seven DAMs, i.e. fourteen actuators are used. The mechanism shown in Fig. 12 can not only achieve high translational acceleration in any

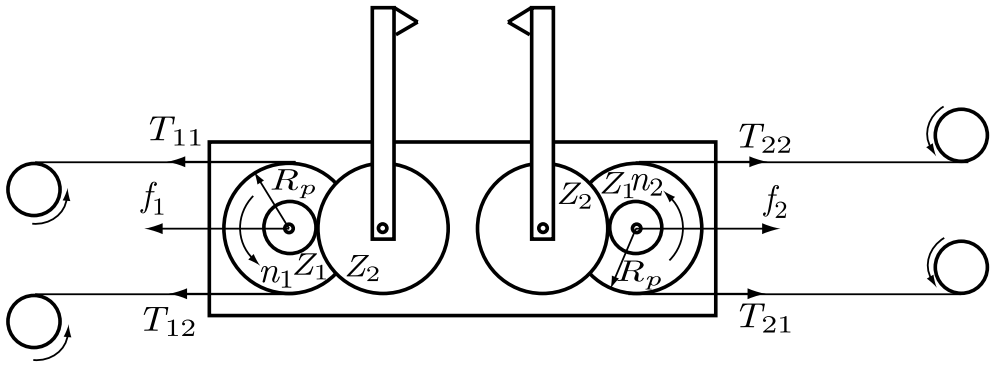

Fig. 11 1D RDWM with local motions

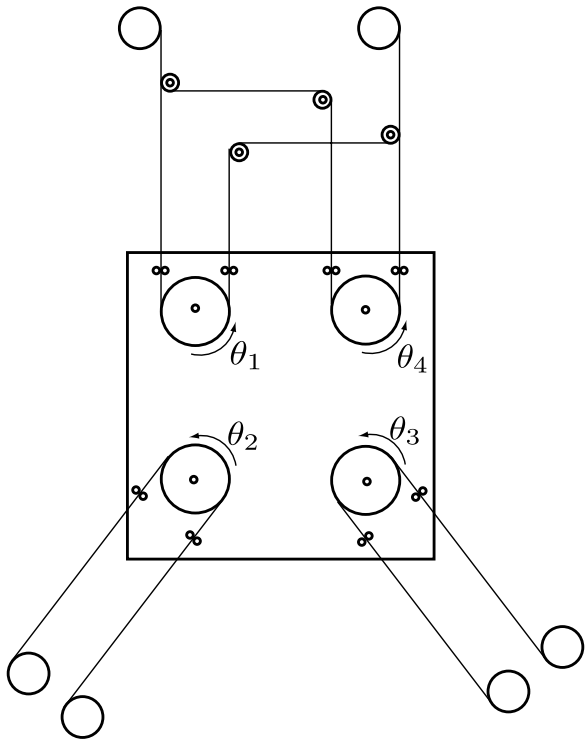

Fig. 12 Illustration of wire mechanism with VCM [18]

direction but can also create local motion by the rotation of pulleys θ_1, θ_2, θ_3, and θ_4. Through these local motions, the robot can change the orientation of the end-effector, as required when performing certain tasks.

Placing the wire inlet on the top plate

When the top plate is moving in the 3D space, the wires can take any direction. A module that can allow the wire to change its directions in response to the posture of the top plate is therefore needed for the operation of RDWM. Figure 13 shows a design of this kind of module. Using this structure, the output part that directs the wire to the actuator unit can produce the ϕ_x, ϕ_y rotations, changing the wire direction in response to the position of the top plate. As the result of using this module, wire can easily be wound onto or out of the DAM and move into or out of the top plate smoothly with small affect of friction.

Conclusions

This paper addresses the configuration of "redundant drive wire mechanisms" (RDWMs) using double actuator modules (DAMs) for producing fast and fine motions. A DAM can contribute to fast motions of the top plate of an RDWM by providing large resultant forces on it, and can produce fine motions of the local mechanisms

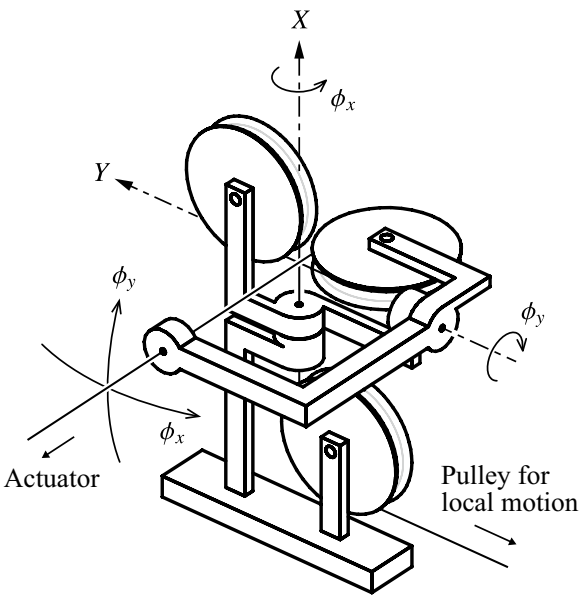

Fig. 13 Example of a wire swing mechanism

mounted on the top plate by providing moments to them. However, designing an RDWM is challenging because DAMs require a large wire matrix to relate the resultant forces and wire tensions, which is used in the vector closure condition. Therefore, this paper has discussed ways of dealing with the vector closure condition of RDWM candidates for investigating the validity of the structure of the candidates. The main results reported in this paper are summarized as follows:

1. The ability of a candidate RDWM to produce resultant forces in any direction can be judged by checking whether the vector closure condition holds for the part of the wire matrix that relates the resultant forces and the combination of the sums of the sets of two wire tensions of the DAMs. This method shows its effect when dealing with multi-dimension RDWM which contains many wires. By using just the essential part and ignoring the whole big size wire matrix, the judgment process becomes very simple, fast and convenient for designers.
2. It is found out that an RDWM has the same structure as a conventional wire mechanism with single actuator modules, where each wire is equivalent to a set of two wires for each DAM in the RDWM, when judging the vector closure condition.
3. The validity of the proposed method was demonstrated by giving examples of the mechanisms in planar and 3D cases that satisfy and do not satisfy the vector closure condition.

The findings obtained in this paper will contribute to conduct the structural design of an RDWM with DAMs.

In future research, a prototype RDWM will be used to experimentally investigate the method for configuring the RDWM discussed in this paper.

Authors' contributions

TNL carried out the study on the proposed judgment procedure, performed analysis of the numerical examples, drafted the manuscript, and revised it. HD helped to establish the proposed judgment procedure, carried out the study on it, provided technical advice, and helped to draft and revise the manuscript. KN designed the study, conceived the proposed judgment procedure, provided technical advice, and helped to draft and revise the manuscript. All authors read and approved the final manuscript.

Acknowledgements

This work was supported by the MEXT-Supported Program for the Strategic Research Foundation at Private Universities, S1311038.

Competing interests

The authors declare that they have no competing interests.

Received: 9 January 2016 Accepted: 27 September 2016
Published online: 18 October 2016

References

1. Kawamura S, Kino H, Won C (2000) High-speed manipulation by using parallel wire-driven robots. J Robot 18:13–21
2. Nagai K, Matsumoto M, Kimura K, Masuhara B (2003) Development of parallel manipulator 'NINJA' with ultra-high-acceleration.IEEE Int Conf Robot Autom 3:3678–3685
3. Nagai K, Nishibu Y, Dake K, Yamanaka A (2009) Design of a high speed parallel mechanism based on virtual force redundancy concept. IEEE Int Conf Ind Technol 1:1–6
4. Higashimori M, Kaneko M, Namiki A, Ishikawa M (2005) Design of 100G capturing robot based on dynamic preshaping. IEEE Int Conf Intell Robot Syst 24(9):743–753
5. Bosscher P, WilliamsII RL (2007) Sebastian Bryson and Daniel Castro-Lacouture: cable-suspended robotic contour crafting system. Autom Constr 17(1):45–55
6. WilliamsII RL, Xin M, Bosscher P (2008) Contour-crafting-cartesian-cable robot system: dynamics and controller design. 32nd Mechanisms and Robotics Conference-ASME. 2: 1–7
7. Alikhani A, Behzadipour S, Alasty A, Vanini AS (2011) Design of a large-scale cable-driven robot with tanslational motion. Robot Comp-Integr Manuf 27(2): 357–366
8. Behzadipour S, Khajepour A (2005) A new cable- based parallel robot with three degrees of freedom. Multi-body Syst Dyn. 13(4):371–383
9. Nagai K, Hanafusa H, Takahashi Y, Bunki H, Nakanishi I, Yoshinaga T, Ehara T (2002) Development of a power assistive device for self-supported transfer motion. IEEE/RSJ Int Conf Intell Robot Syst 2:1433–1438
10. Osumi H, Utsugi Y, Koshikawa M (2000) Development of a manipulator suspended by parallel wire structure. Proceedings 2000 IEEE/RSJ,. 1:498–503
11. Osumi H, Saitoh M (2000) Control of a redundant manipulator mounted on a base plate suspended by six wires. Proceedings 2006 IEEE/RSJ international conference intelligence robots and system. 1:73–78
12. Lampariello R, Heindl J, Koeppe R, Hirzinger G (2006) Reactionless control for two manipulators mounted on a cable-suspended platform. IEEE Int Conf Intell Robot Syst 1:91–97
13. Vischer P, Clavel R (1998) Kinematic calibration of the parallel delta robot. Robotica 16:207–218
14. Pierrot F, Dauchez P, Fournier A (1991) HEXA: a fast six-DOF fully-parallel robot. Adv Robot 2:1158–1163
15. Nagai K, Le Nhat T, Hayashi N, Ito K (2011) Proposal of redundant drive wire mechanism for producing motions with high acceleration and high precision. IEEE/SICE-international symposium on system intergration. p 1049–1054
16. Nagai K, Yoshida H,Yoshimori D (2011) Kinematical analysis of parallel mechanism using multi-wire driven method. J Robot Soc Jpn 29(9):65–72, 2011 **(In Japanese)**
17. Nagai K,Yoshida H, Le Nhat L (2012) Consideration of construction of wire mechanism based on multi-wire driven method. Proceedings of 17th robotics symposia, p 98–103, 2012 **(In Japanese)**
18. Nagai K, Le Nhat T, Hayashi Y, Ito K (2012) Kinematical analysis of redundant drive wire mechanisms with velocity constraint". IEEE/international conference on mechatronics and automation. p 1496–1501
19. Ozawa R, Hashirii H, Yoshimura Y, Moriya M, Kobayashi H (2014) Design and control of a three-fingered tendon-driven robotic hand with active and passive tendons. Auton Robot 36(1-2):67–78
20. Cong Pham B, Yeo SH, Yang G, Kurbanhusen MS, Chen I (2006) Force-closure workspace analysis of cable-driven parallel mechanisms. Mech Mach Theory 41(1):53–69
21. Cong Pham B, Yeo SH, Yang G, Chen I (2009) Workspace analysis of fully restrained cable-driven manipulators. Robot Auton Syst 57(9): 901–912
22. Kino H, Yabe S, Kawamura S (2005) A force display system using a serial-link structure driven by a parallel-wire mechanism. Adv Robot 19(1):21–37